Title: A GT-seq panel for walleye (*Sander vitreus*) provides important insights for efficient development and implementation of amplicon panels in non-model organisms.

Running head: A guide to develop and implement GT-seq SNP panels

Authors: Matthew L. Bootsma[1*], Kristen M. Gruenthal[2], Garrett J. McKinney[3], Levi Simmons[1], Loren Miller[4], Greg G. Sass[5], Wesley A. Larson[6]

Affiliations

[1] Wisconsin Cooperative Fishery Research Unit, College of Natural Resources, University of Wisconsin-Stevens Point, 800 Reserve St., Stevens Point, WI 54481, USA, mbootsma@uwsp.edu, lsimm290@uwsp.edu

[2] Office of Applied Science, Wisconsin Department of Natural Resources, Wisconsin Cooperative Fishery Research Unit, College of Natural Resources, University of Wisconsin-Stevens Point, 800 Reserve St., Stevens Point, WI 54481, USA, kristen.gruenthal@wisconsin.gov

[3] NRC Research Associateship Program, Northwest Fisheries Science Center, National Marine Fisheries Service, National Oceanic and Atmospheric Administration, 2725 Montlake Blvd E, Seattle, WA 98112, USA, garrett.mckinney@noaa.gov

[4] Minnesota Department of Natural Resources, University of Minnesota, 135 Skok Hall, 2003 Upper Buford Circle, St. Paul, MN 55108, USA, loren.miller@state.mn.us

[5] Escanaba Lake Research Station, Office of Applied Science, Wisconsin Department of Natural Resources, 3110 Trout Lake Station Drive, Boulder Junction, WI 54512, USA, gregory.sass@wisconsin.gov

[6] U.S. Geological Survey, Wisconsin Cooperative Fishery Research Unit, College of Natural Resources, University of Wisconsin-Stevens Point, 800 Reserve St., Stevens Point, WI 54481, USA, wes.larson@uwsp.edu

***Corresponding author**

Keywords: Amplicon sequencing, GT-seq, microhaplotype, parentage analysis, genetic stock identification, walleye

Abstract (250 words or less)

Targeted amplicon sequencing methods, such as genotyping-in-thousands by sequencing (GT-seq), facilitate rapid, accurate, and cost-effective analysis of hundreds of genetic loci in thousands of individuals. Development of GT-seq panels is non-trivial, but studies describing trade-offs associated with different steps of GT-seq panel development are rare. Here, we construct a dual-purpose GT-seq panel for walleye (*Sander vitreus*), discuss trade-offs associated with different development and genotyping approaches, and provide suggestions for researchers constructing their own GT-seq panels. Our GT-seq panel was developed using an ascertainment set consisting of restriction site-associated DNA data from 954 individuals sampled from 23 populations in Minnesota and Wisconsin. We then conducted simulations to test the utility of all loci for parentage analysis and genetic stock identification and designed 600 primer pairs to maximize joint accuracy for these analyses. We conducted three rounds of primer optimization to remove loci that overamplified and our final panel consisted of 436 loci. We also explored different approaches for DNA extraction, multiplexed polymerase chain reaction (PCR) amplification, and cleanup steps during the GT-seq process and discovered the following: (1) inexpensive Chelex extractions performed well for genotyping, (2) the exonuclease I and shrimp alkaline phosphatase (ExoSAP) procedure included in some current protocols did not improve results substantially and was likely unnecessary, and (3) it was possible to PCR amplify panels separately and combine them prior to adapter ligation. Well-optimized GT-seq panels are valuable resources for conservation genetics and our findings and suggestions should aid in their construction in myriad taxa.

Introduction

The development of genotyping-by-sequencing (GBS) methods has allowed collection of data from thousands of markers across a genome, enabling research that was not possible using traditional genetic approaches (Davey et al., 2011; Narum et al., 2013). For example, studies using restriction site-associated DNA (RAD) sequencing have shown improved sensitivity for detecting inbreeding depression (Hoffman et al., 2014), increased resolution for determining complex phylogenies (Wagner et al., 2013), and allowed researchers to observe selection on introduced alleles (Bay et al., 2019). Many genetic analyses, however, can be conducted efficiently with genotypes from tens to hundreds of single nucleotide polymorphisms (SNPs) (Anderson & Garza, 2006). Two such approaches that have been widely used in conservation genetics and molecular ecology for decades are parentage analysis and genetic stock identification (GSI).

Parentage analysis involves assigning offspring to putative parents by comparing genotypes at multiple loci, while GSI infers the natal origins of individuals by leveraging allele frequency estimates from baseline populations or reporting groups. These techniques were first conducted using allozyme markers genotyped with protein electrophoresis (Hanken & Sherman, 1981; Milner et al., 1985). Although these analyses were groundbreaking, they often lacked statistical power except in cases of highly diverged stocks or simple pedigrees. The adoption of highly variable microsatellite markers in the 1990s greatly increased statistical power, allowing these two techniques to become widely adopted (Luikart & England, 1999). Despite the advances made possible by microsatellites, problems associated with homoplasy (Garza & Freimer, 1996), locus discovery (Navajas et al., 1998), and reproducibility among laboratories led researchers to explore the potential of biallelic single-nucleotide polymorphisms for GSI and parentage analysis (Seeb et al., 2011).

Although SNPs are less powerful than microsatellites on a per marker basis, SNPs are more abundant in the genome, generally have low genotyping error rates, and can be genotyped using panels capable of efficiently screening a large number of samples (Brumfield et al., 2003; Morin et al., 2004). Early SNP panels were constrained, however, in the availability of molecular markers suitable for genotyping and genotyping costs associated with 5' exonuclease chemistry (Seeb et al., 2011). These constraints were significantly lessened with the proliferation of next-generation sequencing (NGS) technology. For example, methods such as RADseq facilitate quick and affordable discovery of thousands of candidate loci, which can then be selected among for specific purposes.

As SNP discovery has become less expensive, methods of selecting the most informative SNPs for a given study have advanced (Storer et al., 2012). Previous research has shown that information content will vary among SNPs depending on the context within which they are applied and location within the genome (i.e. coding or non-coding regions). For example, Ackerman et al. (2011) found that SNPs under diversifying selection provide increased accuracy and precision in GSI of sockeye salmon (*Oncorhynchus nerka*) from the Copper River, Alaska. In general, previous studies have shown that GSI accuracy is generally positively correlated with differentiation (e.g., F_{ST}) and, to a lesser extent, diversity (e.g., heterozygosity) (Ackerman et al., 2011; Bradbury et al., 2011; Storer et al., 2012). Studies of SNP selection methods for parentage analysis, however, have found that high diversity is the most important attribute to consider when creating a panel (Baetscher et al., 2018). More recently, analytical techniques have shifted towards consideration of closely linked SNPs (i.e. microhaplotypes), which effectively increases the diversity at a locus and has proven useful for parentage and GSI tests (Baetscher et al., 2018; McKinney, Seeb, et al., 2017; Reid et al., 2019). While obtaining microhaplotypes would require independent assays for each SNP at a locus using previous 5’ exonuclease methods, NGS technology has enabled the joint genotyping of multiple SNPs within single reads, making microhaplotype data easily obtainable through a simple modification in analytical approach.

In addition to increasing the volume of molecular markers sampled, NGS technology also facilitates increased throughput with respect to the number of individuals genotyped. This is especially true for amplicon sequencing approaches, which generally utilize highly-multiplexed polymerase chain reaction (PCR) to genotype many individuals and loci on a single high-throughput sequencing lane. Amplicon sequencing approaches do not require an allele-specific probe, can genotype multiple SNPs within an amplicon using a single primer pair, and are generally significantly less expensive than 5’ exonuclease chemistry, especially in the context of genotyping thousands of individuals. Many amplicon sequencing approaches exist, and most large biotechnology companies offer a unique amplicon sequencing solution (e.g. Illumina TruSeq, ThermoFisher Ion AmpliSeq). However, these solutions can be expensive, and often lack the flexibility desired by conservation geneticists. For example, many companies do not support multiplexing of thousands of individuals within a single sequencing lane.

One recently developed amplicon sequencing method that provides a more cost-effective and flexible workflow is genotyping-in-thousands by sequencing (GT-seq). This amplicon sequencing method, which was developed by Campbell et al. (2015), facilitates the creation of custom panels containing hundreds of SNPs that can be genotyped in thousands of individuals on a single high-throughput sequencing lane. As noted above, GT-seq is one of many amplicon sequencing approaches but has already shown great promise for conservation genetics applications (reviewed in Meek and Larson 2019). Here, we focus on GT-seq and suggestions for optimizing the GT-seq workflow rather than comparisons between GT-seq and other amplicon sequencing methods (e.g. Chen et al., 2016; Onda et al., 2018) as those comparisons could warrant a full manuscript.

Despite its benefits, GT-seq is not yet widely used outside of salmonids. Early applications to non-model organisms, however, have shown great promise for this method's versatility, including the ability to reveal dispersal and mating patterns in a complex environment (Baetscher et al., 2019), provide insight to the ecological and evolutionary dynamics of secondary contact (Reid et al., 2019), and understand population diversity in systems that are heavily influenced by climate change (Pavinato et al., 2019). Pedigree analysis in wild populations relies particularly heavily on the ability to genotype large sample sizes to increase the likelihood of detecting kin relationships, toward which GT-seq is ideally suited. Moreover, GT-seq has proven capable of generating high-quality genotypes from low-quality DNA samples (Natesh et al., 2019; Schmidt et al., 2019), making it a viable approach for monitoring endangered or elusive species.

While GT-seq panels have been developed to maximize accuracy for GSI (McKinney et al., 2019) or parentage (Baetscher et al., 2018) analyses, the potential for developing dual-purpose panels is largely unexplored. Moreover, developing GT-seq panels is a relatively involved task and, to this point, while there are papers describing panel development (Baetscher et al., 2018; Campbell et al., 2015; McKinney et al., 2019), there are limited resources providing guidelines and suggestions for efficient panel construction. For example, there are many decision points in panel development related to primer selection, multiplexing approaches, laboratory protocols, and analysis parameters that have yet to be addressed. We used walleye (*Sander* *vitreus*) from Minnesota and Wisconsin as a test case to investigate various tradeoffs associated with GT-seq panel development and optimization and leveraged our collective experience to provide guidelines for researchers developing GT-seq panels.

Walleye are an apex predator and one of the most prized sportfish throughout their native and introduced range. Recently, many walleye populations have declined across the Midwestern United States (Embke et al., 2019; Hansen et al., 2015; Rypel et al., 2018), prompting increases in stocking efforts relative to already large and long-term regional stocking programs that have existed for decades. Genetic studies have been used to guide these efforts by informing broodstock selection and general stocking practices. Genetic variation in walleye from this region was first characterized by Fields et al. (1997), who found geographic-based patterns of genetic structure, but limitations related to sample size and molecular marker choice resulted in the use of contemporary watershed boundaries as genetic management units. This research was later expanded upon by (Hammen & Sloss, 2019), who attempted to further define genetic structure in the Ceded Territory of Wisconsin (approximately the northern third of the state) and test whether significant genetic structure existed between distinct hydrological basins within this region. Once again, constraints associated with available molecular markers used in a system with not only low differentiation, but also extensive stocking precluded definition of fine scale structure. This system, however, provides an excellent model for applying genomic techniques to discriminate populations and evaluate hatchery programs using parentage analysis.

Like many intricacies of genomics research, GT-seq panel development is a process that is at once broadly generalizable to non-model organisms and highly specific to the taxa it is applied to. While the overarching steps (Fig. 1) will remain constant, there are many decision points within that will require informed thought and decision. Here, we used walleye, a species with few well-established genomic resources, as a model to examine the methods inherent to GT-seq panel development, identify critical decision points in the process, and illuminate the nuances associated with them. Our overarching goal was to design a dual-purpose GT-seq panel optimized for parentage analysis and GSI in walleye. The creation of this panel allowed us to address the following specific objectives: (1) investigate the tradeoffs between choosing markers for parentage analysis versus GSI, (2) explore the most efficient way to design an optimized panel, and (3) evaluate various laboratory approaches to maximizing the efficiency of GT-seq genotyping. We provide an in-depth discussion of our experiences designing the panel and outline important topics that should aid researchers in designing future GT-seq panels.

Materials and Methods

Sample collection

Tissue samples were collected from adult walleye from 23 inland lakes across Wisconsin and Minnesota and the St. Louis River (border water) (Fig. 2a, Table 1) and stored in 95% ethanol until DNA extraction. We obtained samples from as many major drainages as possible across the two states, with an emphasis on the Wisconsin and Chippewa River drainages in Wisconsin, which were difficult to differentiate using microsatellites (Hammen & Sloss, 2019). In Minnesota, sampling focused primarily on major sources of wild broodstock for stocking programs. Samples were collected by the Wisconsin and Minnesota Departments of Natural Resources using fyke nets or electrofishing. Sampling took place during the spring spawning runs of April 2015 and 2017 and fall surveys in August and September of 2015 and 2017. Stocked individuals may be tagged, or fin clipped; we inspected all sampled individuals for tags or fin clips to avoid as many individuals as possible that were of stocked origin.

Preparation of RAD sequencing libraries

Genomic DNA was extracted in a 96-well format with Qiagen DNeasy Blood and Tissue Kits. Extracted DNA was quantified using a Quant-iT PicoGreen dsDNA Assay Kit (Invitrogen, Waltham, MA) and normalized to 20ng/µl. We then prepared DNA for RADseq library preparation following the BestRAD protocol (Ali et al., 2016). Briefly, DNA was digested in a 2 µl reaction with the restriction enzyme *SbfI*, and biotinylated barcode adaptors were ligated to the 5' cut ends. Shearing of DNA was conducted using a 12.5 µl fragmentase reaction. Library preparation was conducted using an NEBNext Ultra DNA Library Prep Kit for Illumina (NEB, Ipswich, MA), with a 12-cycle PCR enrichment. We then inspected RAD library quality on a 2% agarose gel before undergoing a final AMPure XP (Beckman Coulter, Indianapolis, IN) purification and quantification on a Qubit 2.0 Fluorometer (HS kit, ThermoFisher Scientific, Waltham, MA). Libraries were sequenced using paired-end (PE) 150 technology on a HiSeq 4000 (Illumina, San Diego, CA) at the Michigan State University Genomics Core Facility or Novogene Corporation, Inc. (Davis, CA). Sequencing was conducted to achieve a target of over one million retained reads per individual.

Analysis of RAD data to discover SNPs

Loci were identified and genotyped in STACKS v.2.2 (Rochette et al., 2019) without using gapped alignments. Raw reads were demultiplexed and barcodes were trimmed in *process_radtags* (parameter flags: -e *SbfI*, -c, -q, -filter_illumina, -r, --bestrad). We assembled RAD-tags into putative RAD loci with *ustacks* using the bounded model (bound_high = 0.05, --disable-gapped) and allowing for a maximum of three nucleotide mismatches (-M = 3) and four stacks per locus (-max_locus_stacks = 4), as well as a minimum depth of three (-m = 3). The calling of haplotypes from secondary reads was disabled (-H). A catalog of consensus loci was assembled in *cstacks* using the two individuals with the highest number of retained reads from each population, allowing a maximum of three mismatches between sample loci (n = 3, --disable-gapped). After matching all samples against the catalog in *sstacks* (--disable-gapped), data were oriented by locus with *tsv2bam*, and individual genotypes were called in *gstacks*, with paired-end reads incorporated. Genotypes were exported in variant call format (vcf) using *populations*, with loose filtering parameters (SNPs present at >5% of individuals, minimum minor allele frequency of >0.005).

Comprehensive filtering of individuals and genotypes was conducted in vcftools v0.1.15 (Danecek et al., 2011) by: 1) removing individuals missing >20% of SNP calls, 2) removing SNPs that were missing in >20% of individuals, and 3) removing SNPs that were not in the first 140 base pairs of the RAD-tag. This filtering effectively reduced the dataset to include SNPs detectable using single-read (SR) 150 sequencing to simplify downstream amplicon design. Putative duplicated loci were identified in HDplot (McKinney, Waples, et al., 2017) ($H > 0.5$, $-7 < D < 7$) and removed with vcftools. Retained individuals and SNPs were used to form whitelists for input into *populations* that output a filtered vcf of multi-SNP haplotypes, which was then filtered to remove loci with more than 10 alleles and used in simulations for locus selection. We also estimated single-SNP F_{IS} across all populations using diveRsity v1.9.90 (Keenan et al., 2013) and excluded any SNPs with F_{IS} values >0.2 or <-0.2 from locus selection. Loci with more than 10 alleles likely represent duplicated or repetitive sequences that are found in many places throughout the genome, and loci with highly positive or negative F_{IS} values may indicate null alleles or high heterozygosity resulting from duplicated or repetitive sequences. Finally, loci with a SNP in the first 10 base pairs of the RAD-tag were excluded to allow room for forward primer design.

Analysis of population structure, locus selection, and panel assessment

To understand population structure in our system and ensure that selected loci could facilitate accurate parentage assignment and GSI, we evaluated patterns of genetic divergence using pairwise F_{ST} (Table S1) estimated in Arlequin v3.5.2 (Excoffier & Lischer, 2010) and constructed a dendrogram (Fig. 2b) using Nei's distance in poppr v2.8.2 (Kamvar, Tabim, & Grünwald, 2014). These analyses facilitated identification of population pairs that would be challenging to discriminate and supported historic data suggesting several populations were founded from hatchery sources located outside of their drainage basin (Escanaba Lake, Sanford Lake, and Lake Millicent in Wisconsin); these populations were removed from simulations of panel accuracy to ensure that selected loci would best represent the natural genetic patterns of the region.

After initial population genetic analyses, loci were selected for primer development by constructing several test panels from the RAD data and simulating assignment accuracy for parentage and GSI. Previous research suggested that choosing loci with greater genetic differentiation (e.g., F_{ST}) should maximize accuracy for GSI (Ackerman et al., 2011; Storer et al., 2012), while choosing loci with higher diversity (e.g., heterozygosity and number of alleles) maximizes accuracy for parentage (Baetscher et al., 2018). We therefore constructed the test panels using single-SNP F_{ST} estimated in diveRsity v1.9.90 (Keenan et al., 2013) as well as expected heterozygosity at a multi-SNP haplotype ($H_{\mathrm{E\_mhap}}$) and the number of alleles at a locus estimated in adegenet v2.1.1 (Jombart & Ahmed, 2011). All simulations were conducted with genotypes coded as multi-SNP haplotypes.

GSI accuracy for each panel was assessed via 100% simulations implemented in rubias (Moran & Anderson, 2018) using the *assess_reference_loo* function (mixsize = 200, reps = 1000). Populations were aggregated into reporting units based on hydrological basins (Table 1).

Collections within a simulation were drawn from a Dirichlet distribution with all parameters equal to 10 (i.e., each simulation's prior contained approximately equal proportions of each population for the given reporting unit). Individuals were assigned to reporting groups if they had a cumulative probability of >70%, a typical value for studies conducting individual assignment to reporting groups or populations (Ackiss et al., 2020). Unfortunately, limited sample sizes in some reporting units prevented creation of separate training and holdout datasets as suggested by Anderson (2010), thus assignment accuracies presented here may be upwardly biased and would need to be reassessed more thoroughly for populations involved in an applied study.

We assessed the power of each panel for assigning parentage and other kin relationships in CKMRsim (Anderson, https://zenodo.org/record/820162), which employs a variant of the importance sampling algorithm of (Anderson & Garza, 2006) that allows for more accurate estimates of a very small false-positive rate (per-pair rate of truly unrelated individuals being inferred as related) versus those obtained using standard Monte Carlo methods (Baetscher et al., 2018). Parentage analyses were conducted following the methods of Baetscher et al. (2018), whereby log-likelihood ratios between a tested relationship and the hypothesis of no relationship are computed from the calculated probabilities of genotype pairs for related individuals simulated from allele frequency estimates. Distributions of simulated log-likelihood ratios are then used to compute false-positive rates. Using this approach, we estimated false-positive rates for parent-offspring, full-sibling, and half-sibling relationships at false-negative rates (per-pair rate of truly related individuals being inferred as unrelated) ranging from 0.01 to 0.1.

Panels of 600 unique loci were iteratively selected, choosing loci based first on rank F_{ST} then rank $H_{\mathrm{E\_mhap}}$, and their utility was tested by conducting GSI tests and parentage simulations. We targeted 600 loci because previous published (McKinney et al. 2019) and unpublished studies in salmonids have suggested that attempting to include more than 400-500 loci in a GTseq panel can lead to primer interactions that prevent efficient genotyping. We ultimately defined three panels of 600 loci that best described the tradeoffs between markers selected based on F_{ST} and heterozygosity. Loci in these panels were chosen by selecting 1) the top 600 loci based on F_{ST}, 2) the top 300 loci based on F_{ST} and 300 based on H_{E_mhap} (If a locus was present in both lists [n = 12] it was allocated to the F_{ST} list, and the next rank H_{E_mhap} locus was selected), and 3) the top 600 loci based on H_{E_mhap}. These panels are hereafter referred to as F_{ST_600}, Composite$_{\_600}$, and Diversity$_{\_600}$, respectively. Through further testing, we determined that a variation of the Composite$_{\_600}$ panel, with 250 loci based on H_{E_mhap} and 350 loci based on F_{ST} performed slightly better for GSI and parentage analyses than a panel with 300 markers from each category and proceeded to design primers for the selected loci. While choosing equal numbers of markers from each category is logistically simpler, we encourage researchers designing similar panels to test different combinations of markers from each category in order to maximize assignment power.

Primer Design

To design PCR primers for the selected loci, their consensus sequences were subset from the STACKS catalog into a FASTA file for import into Geneious Prime® 2019.1.1 (https://www.geneious.com). The freeware program Primer3 (Untergasser et al., 2012) can also be used, although it lacks a graphical user interface. The vcf file produced in the vcftools step containing all SNPs and alleles within a consensus sequence was included to ensure primers were properly designed (i.e., should a SNP fall within a primer binding region, a degenerate nucleotide could be inserted or the primer re-designed). Primer pairs were iteratively designed, with optimal target parameters defined as a primer length of 20 bp, product size of 140 bp to facilitate genotyping with SR chemistry, Tm of 60° C, GC content of 50%, and no more than four of the same base repeated consecutively (i.e., poly-X repeats). Primers identified as matching one or more off-target sites, which could lead to amplification of multiple products, were redesigned. Given that not all 600 candidate loci initially identified were suitable candidates for primer development, we continued to iteratively select loci and design associated primers until we reached our target of 600 loci. Assignment accuracy for the 600 loci we successfully designed primers for was then assessed via simulation. Unfortunately, the loci selected for primer design were based on data containing a subset of individuals with discordant encoded and true identities as a result of transposition of *in-silico* barcodes during demultiplexing. Despite these discrepancies, the effect was likely minor as only 8% of individuals were incorrectly assigned to reporting units prior to simulation. Simulation results shown here were conducted using corrected data.*GT-seq optimization*

Sequencing via GT-seq was conducted following the methods of Campbell et al. (2015), with modification to the multiplex thermal cycling conditions (95 °C hold for 15 min; five cycles of 95 °C for 30 s, 5% ramp to 57 °C for 2 min, 72 °C 30 s; and 10 cycles of 95 °C for 30 s, 65 °C for 30 s, and 72 °C 30 s) and post-normalization dual-sided SPRI size-selection and purification (0.6X plus 0.4X) to further restrict the product size range (e.g., primarily toward removal of primer inter-hybridization). Final library quality control consisted of confirmation of amplification and barcoding by SYBR Green-based RT-qPCR (Stratagene Mx3005P QPCR System, Agilent, Santa Clara, CA), visualization on a 2% agarose E-Gel (Invitrogen, Carlsbad, CA), and quantification using picogreen. Libraries were then sequenced at the University of

Wisconsin-Madison Biotechnology Center (UWBC) DNA Sequencing Facility on a MiSeq (Illumina) using 2 × 150 bp flowcells.

Demultiplexed amplicon sequencing data were processed using *GTscore v1.3* (McKinney et al., 2019). *GTscore* generates *in-silico* primer-probe sequences from a catalog of loci generated in STACKS, that are then matched to amplicon sequences and call genotypes for individual SNPs as well as multi-SNP haplotypes. *GTscore* also enables separation of on-target sequence reads (i.e., reads containing both an *in-silico* primer and associated probe) from reads produced as a result of primer cross-hybridization. Primer-probe file development was accomplished with *sumstatsIUBconvert.pl* by obtaining the IUB code information for each SNP from the sumstats.tsv file produced in the STACKS pipeline, converting catalog sequences produced in the STACKS pipeline to FASTA sequences using *catalog2fasta.pl*, and merging IUB code information with the catalog.fasta using *fasta2IUB.pl*. This primer-probe file was then input for *AmpliconReadCounter.pl*, along with an individual's fastq file, to produce read count summaries of primers and probes.

Overall, we conducted three rounds of panel optimization to identify and remove loci that had disproportionately high amplification rates (i.e., "overamplifiers") and ensure that our panel was capable of delivering a high proportion of on-target reads for each locus as well as homogeneous amplification rates among loci. The first round of optimization used DNA from a single walleye from Sanford Lake, WI, while the second and third rounds were conducted on subsets of 24 individuals from each of four populations (96 individuals total) originally included in the RADseq study: Delavan Lake, Medicine Lake, and the Wolf River in Wisconsin and the Pine River in Minnesota. Upon completing the final optimization, the characteristics of retained loci were compared to those of loci culled from the panel. This was done by performing a

Welch's two sample t-test ($\alpha = 0.05$) between the GC:AT ratio of primers that were retained and those culled and between the GC:AT ratio of DNA templates retained and culled, based on the first 140 bp of the template as this was the region in which SNPs were targeted. We also assessed the assignment accuracy of the fully optimized panel by performing GSI and kinship simulations with the retained loci.

Sequenced GT-seq libraries from each round were collectively analyzed for PCR accuracy and uniformity. Accuracy was measured by calculating the proportion of reads containing *in-silico* primer sequences (total reads) relative to those that also contained *in-silico* probes. Uniformity of amplification among loci was determined by calculating the proportion of total reads that were allocated to the top 10% of loci, based on locus read counts (prop_reads_T10); if amplification was perfectly uniform across loci, we would expect prop_reads_T10 to account for exactly 10% of total reads. Given that amplification rates vary substantially within a panel, we compared among locus performance by plotting the relative $\log_{10}$ abundance of total and on-target reads at each locus in descending order, which facilitated visual identification of overamplifiers. As among-locus amplification rates evened out after the first optimization, the on-target proportion of reads at each locus became a factor in retaining or excluding loci during the second optimization.

Testing methodological modifications and performance analysis

During panel optimization, we compared the quality of GT-seq libraries prepared from DNA extracted with Qiagen DNeasy and a more cost-effective chelating resin-based procedure. Performance of libraries was compared using Bonferroni corrected ($\alpha = 0.016$) Tukey's HSD for the number of on-target reads and the proportion of total reads that were on-target, after determining whether significant differences existed among libraries via a one-way ANOVA (α = 0.05). DNA was extracted from the 96 test individuals twice, first using Qiagen DNeasy and again with a 10% Chelex 100 (200-400 mesh; Bio-Rad, Hercules, CA) solution containing 1% each of Nonidet P-40 and Tween 20 (Millipore Sigma, St. Louis, MO). Additionally, we compared results with and without the exonuclease I and shrimp alkaline phosphatase (ExoSAP) procedure included in (Campbell et al., 2015) to remove PCR inhibitors and free nucleotides. Therefore, we conducted GT-seq on all individuals in triplicate: 1) Qiagen with ExoSAP, 2) Chelex with ExoSAP, and 3) Chelex without ExoSAP, and all tests were sequenced on the same MiSeq lane. Finally, we also tested whether the total number of loci successfully targeted could be increased through methodological adjustments. We accomplished this by dividing our optimized primer panel into two non-overlapping primer pools before multiplex PCR amplification. We then merged PCR products from the separate pools prior to the barcoding PCR. The sequencing performance of this joint panel was then compared to the single multiplex containing the full panel using a Welch's two sample t-test (α = 0.05).

We examined genotype concordance between RADseq and GT-seq across GT-seq read depths using the fully optimized panel in the third round. Genotypes were called using *PolyGen* (McKinney et al., 2018), an extension of the *GTscore* pipeline that uses the same maximum-likelihood algorithm as STACKS v1 for diploid, bi-allelic loci. The average coverage of RADseq data at GTseq loci retained for these comparisons was 26.55, which is typical for many RAD studies (Euclide et al., 2020). However, genotyping error rates at these moderate read depths are still relatively common (Nielsen et al., 2011). Therefore, we only retained genotypes if they had greater than 60× coverage in RADseq data to minimize the chances that genotyping discrepancies were caused by incorrect RAD genotypes. We then modeled the relationship between GT-seq read depth and genotype concordance using only read depths with more than 30 genotypes to ensure that estimates of genotype concordance at a given depth had adequate sample sizes.

As a final proof of concept, we tested the optimized panel on a sample of 570 walleye obtained from Escanaba Lake, WI, using the methods described above to estimate the variance in read depth among loci within a pool. We retained only loci present in more than 70% of individuals and individuals genotyped at more than 70% of loci.

Results

Analysis of ascertainment dataset

A total of 954 individuals from 23 populations were RAD sequenced, with an average of 42 individuals per population (Table 1). Sequencing yielded 1,313,358 retained reads on average per individual (range = 8,941 - 8,176,163). Initial sequence data was used to identify 682,223 putative SNPs. After passing sequence data through quality filters, 839 individuals and 20,597 SNPs were retained (Table S2).

Population estimates of H_O (0.144 - 0.179), allelic richness (1.498 - 1.674), and F_{IS} (-0.050 - 0.017) were relatively similar across locations (Table 1). Populations from Minnesota had slightly lower diversity, which may be due to ascertainment bias as 14 of the 23 populations were from Wisconsin. The highest genetic differentiation was observed between populations from Minnesota and Wisconsin, with further structuring by drainage basin within each state (Fig. 2b, Table S1). Structuring was higher in Minnesota, with most populations showing a relatively high degree of isolation (average F_{ST} = 0.07, Table 2). Structure in Wisconsin was shallower (average F_{ST} = 0.03, Table 2) and only loosely correlated with drainage basins. From these results, we constructed 13 reporting groups to facilitate GSI to identifiable genetic units (Table 1). All the reporting groups from Minnesota contained single populations, whereas in Wisconsin, while the Rock-Fox and Wolf River groups contained single populations, the Wisconsin and Chippewa River groups each contained five populations. Some single populations in the Wisconsin and Chippewa Rivers were distinctly identifiable (e.g., Eau Claire River, Medicine Lake), but we grouped these populations within their drainage basin of origin as the panel will likely be used this way for management purposes.

Locus selection and panel assessment

GSI accuracy was similar among the three panels, with < 1% difference in average accuracy between the panel with loci chosen based solely on differentiation (F_{ST}_600) and the panel based solely on diversity (Diversity_600) (Fig. 3, Table 3). Average assignment accuracy was > 90% for nine of the 13 reporting units in all panels (Fig. 3a). The remaining four reporting units had average assignment accuracies ranging from 78% to 86%. Three of these units (upper Chippewa River, WI; St. Louis River, MN/WI; and Red Lake, MN) are known to have admixed stocking histories (personal communications with Wisconsin and Minnesota Departments of Natural Resources biologists), while the fourth, North Fork Crow River, MN, included Lake Koronis, which had the fewest individuals retained after filtering (n = 15). Misassigned individuals from the St. Louis River, MN, and Red Lake, MN groups primarily assigned to the Pike River, MN, an unsurprising result given that fish from the Pike River contributed to the recovery of the collapsed walleye fishery in Red Lake (Logsdon et al., 2016) and fish in the St. Louis River watershed. Misassignments from the Upper Chippewa basin primarily assigned to the Upper Wisconsin basin due to the lower differentiation described previously.

The populations with the lowest assignment accuracies were found in the Chippewa River and Wisconsin River reporting groups (Table S3, S4, S5), particularly in northern Wisconsin near the headwaters of the Chippewa and Wisconsin River drainages, and included

Big Arbor Vitae Lake (F_{ST_600} accuracy = 74%), Manitowish Lake (F_{ST_600} accuracy = 58%), and Turtle Flambeau Flowage (F_{ST_600} accuracy = 63%). A large portion (> 10%) of the simulated individuals from these populations could not be assigned to any population, providing further support for the genetic similarity of these two reporting groups. A high proportion of individuals from Big Arbor Vitae Lake were assigned to Manitowish Lake (12%) and vice versa, from Manitowish Lake to Big Arbor Vitae Lake (20%). Most misassignments in the Turtle Flambeau Flowage were to Kawaguesaga Lake (16%). Populations with high misassignment rates also tended to have short branch lengths in the dendrogram and were often located near the root of a clade (Fig. 2b). Furthermore, the two populations from the upper Chippewa basin (Manitowish Lake and Turtle Flambeau Flowage) had lower pairwise F_{ST} values, on average, with populations from the upper Wisconsin than the upper Chippewa.

The Diversity$_{\_600}$ panel had the highest accuracy for assigning kin relationships, the Composite$_{\_600}$ panel showed intermediate performance and the F_{ST_600} panel had the lowest accuracy rate (Fig. 3b, Table 3). For all panels, false-positive rates were < 10^{-20} for parent-offspring and full-sibling relationships, indicating all panels would perform adequately for reconstructing most relationships in most study systems. Inter-panel performance did, however, range widely, from a false-positive rate of 4.68 × 10^{-34} for F_{ST}_600 to 2.74 × 10^{-80} for Diversity$_{\_600}$ panel at a false-negative rate of 0.01. Within panels, false-positive rate was inversely related to false-negative rate.

Primers were designed using a modified Composite_600 panel, with 250 loci chosen based on $H_{\mathrm{E}\_\mathrm{mhap}}$ and 350 chosen based on F_{ST}, as this panel delivered the best joint accuracy for GSI and kinship analyses (Fig. 3, Table 3). Of the initial 600 loci initially selected for primer design, 100 were not suitable for primer design, and thus, iterative selection of loci meeting primer design requirements was continued until the targeted number of F_{ST} and diversity markers was met.*GT-seq optimization*

Initial amplification and MiSeq sequencing of all 600 loci yielded 4,655,071 reads containing intact i7 barcode sequences, with 4,150,910 reads (89%) matching *in-silico* primer sequences. Locus specificity was considered via the proportion of total reads that were on-target, which was 1,031,707 (24%) (Table 4). In terms of amplification uniformity among loci, prop_reads_T10 accounted for 3,526,201 (85%) of the 4,150,910 total reads. A cutoff of 3,000 reads per locus was then visually identified (Fig. 4a); loci producing more than 3,000 reads (n = 123) were deemed overamplifiers and discarded prior to further optimization.

For the second round of optimization, the remaining 477 primers pairs produced 12,653,262 reads containing intact i7 barcode sequences, and 9,347,591 (74%) matched *in-silico* primer sequences. Locus specificity improved, with 3,268,293 (35%) of the total reads successfully aligning to *in-silico* probe sequences (Table 4). Improvement was also observed in the uniformity of amplification across loci, with prop_reads_T10 equating to 72% (6,776,302) of total reads. Because locus performance was less variable in this round of testing, the individual on-target proportion of reads at a locus was also considered while culling undesirable loci. As such, loci visually identified as overamplifiers were again discarded if they did not display high on-target read proportions (n = 41, Fig. 4b).

The third GT-seq test was used to determine the functional performance of the panel and aimed to target 858 SNPs across 436 loci (Fig. 4c). This test produced 7,282,101 reads with intact i7 barcodes, and 6,827,424 (94%) matched to *in-silico* primers. Locus specificity of primer pairs improved greatly in this test, as 6,262,523 (92%) of the total reads were also on-target

(Table 4). Likewise, the variation in amplification rates across loci decreased as evidenced by prop_reads_T10 decreasing to 37% (2,148,932) of the total reads.

Upon completion of panel optimization, a small but significant difference was observed between the GC content of primers that were retained (mean = 49.2%) and primers that were removed (mean = 51.4%, df = 602, t = 5.4, $p < 0.001$). Similar differences were found when comparing the GC content of the DNA template; significantly higher GC proportions were present in templates that were culled from the panel (mean = 47.8%) than templates that were retained (mean = 45.5%, df = 359, t = 3.8, $p < 0.001$). Additionally, a total of 88 primer pairs in the original panel contained at least one degenerate nucleotide, 72 (81%) of which were in the forward primer. After optimization, 56 of the initial 88 primer pairs (64%) were retained. In comparison, of the 512 initial primer pairs that did not have degenerate primers, 380 (74%) were retained.

The average F_{ST} for the most informative SNP at a locus and the average $H_{\mathrm{E\_mhap}}$ did not change appreciably between the initial and fully optimized panels (Table 4). Similarly, assignment accuracy showed minimal differences between GSI simulations performed using the final 436 loci and the initially selected 600 (0.6% difference in accuracy on average, Fig. S1. Kinship assignment error rates, which were the most variable in initial simulations, showed an increase of approximately 1×10^{-10} for both parent-offspring and full-sibling relationship assignment after optimization (Fig. S1). False-positive rates for parent-offspring assignment did, however, remained below 1×10^{-20} at a false-negative rate of 0.01, indicating that the ability to identify parent-offspring relations in most systems was still high. Likewise, false-positive rates for identifying full-sibling relations (4.92×10^{-18} at a false-negative rate of 0.01) retained sufficiently low error rates for the panel to perform this task.

Methodological modifications and performance analysis

Significant differences for on-target read counts and the proportion of total reads that were on-target were detected among genomic DNA extraction and purification method combinations. Subsequent analysis using Tukey's HSD revealed that Chelex-extracted DNAs produced the highest on-target read count, and Qiagen-extracted DNAs with ExoSAP-purification produced the lowest (Fig. 5, $p < 0.001$). While the proportion of on-target reads did not differ between Chelex with ExoSAP and Qiagen with ExoSAP, both methods produced a significantly lower proportion of on-target reads than the Chelex-only library (Fig. 5, $p < 0.001$). Although we did not test Qiagen-extracted DNAs without ExoSAP, analysis in our laboratory on other species suggests this approach performs similarly to Chelex without ExoSAP. When comparing results from the full panel of 436 primer pairs to those obtained using the same panel divided into two unique multiplexes of 209 and 227 primer pairs (n = 436) and repooled prior to barcoding, no significant differences were found in total primer reads (df = 860, t = 0.10, p = 0.92), on-target reads (df = 858, t = 0.16, p = 0.87), or the proportion of total reads that were on target (df = 806, t = 0.66, p = 0.51).

A total of 4,063 genotypes across 406 loci (820 SNPs) could be used in comparisons between GT-seq data and those obtained from the original RAD study. Of these genotypes, 96.6% of calls were identical between methods, and modeled expectations of genotype concordance (residual sum of squares = 0.02) indicted that a concordance rate of 99.0% could be expected at a GT-seq read depth of 31 (Fig. 6).

For a final proof of concept, a new sample of 570 walleye was sequenced using the current panel of 436 loci. After filtering, 551 individuals and 303 loci were retained with an average of 32.9 (SD = 29.1) reads per locus; 116 of the 303 loci exhibited an average coverage greater than the 31× target identified for 99% genotyping concordance (Fig. 7) The average percent missing data was 6.4% (SD = 13.0%) across individuals and 30.0% (SD = 38.0%) across loci.

Discussion

Amplicon sequencing methods such as GT-seq have tremendous potential for facilitating high-throughput genotyping in non-model organisms (Meek & Larson, 2019). Few published studies, however, have critically analyzed the panel development process (see McKinney et al. 2019). Here, we leverage our experiences developing a GT-seq panel for walleye with testing various aspects of the GT-seq methodological process to provide general guidelines usable by other researchers to simplify panel construction and validation, particularly in non-model species. Our walleye panel has the necessary power to conduct GSI in a study system with highly variable degrees of genetic differentiation and perturbation by historical stocking, while also being capable of identifying parent-offspring and full-sibling relationships within large populations. In fact, this panel has already been screened on over 2,000 additional walleye in Wisconsin, providing valuable information on out-of-basin stockings as well and survival of stocked fish inferred from parentage analysis (data not shown). The robust performance of our panel was facilitated by exploring the upper limits of how many loci a GT-seq panel can target and the trade-offs between choosing loci for GSI versus parentage analysis. The guidelines and suggestions presented here will aid in the efficient creation of multipurpose GT-seq panels in organisms with little to no available genomic resources.

Patterns of population structure: historic stocking influences GSI accuracy

The largest genetic differentiation in our data was observed between populations from Wisconsin and Minnesota; this structure was likely the result of recolonization from different refugia following the Wisconsin glaciation, which ended ~10,000 years ago. A range-wide analysis of walleye genetic structure using microsatellite loci produced similar patterns, with the most genetically independent populations found in northern Minnesota and Canada (Stepien et al., 2009). Additionally, we found that while populations in Minnesota displayed strong isolation on relatively small spatial scales, broad-scale patterns of isolation were less evident in Wisconsin. In particular, the Ceded Territory of Wisconsin (CTWI), which included our Chippewa River and Wisconsin River reporting groups, displayed patchy and low genetic structure overall. It is likely that structure in this region has been compromised by stocking. Hammen and Sloss (2019), for instance, observed that several populations of walleye in the upper Chippewa were more genetically similar to populations in the upper Wisconsin than to other populations in the upper Chippewa, while nongame species in the CTWI displayed patterns of genetic divergence strictly associated with drainage basin boundaries (Westbrook, 2012). We also observed that four proximate populations spanning the Chippewa and Wisconsin River boundaries were nearly indistinguishable (Turtle Flambeau Flowage, Manitowish Lake, Kawaguesaga Lake, Big Arbor Vitae Lake). These populations are within 50 km of each other and are located near a state walleye hatchery in Woodruff, WI, that has historically used broodstock solely from the Wisconsin River drainage basin (personal communication, Steve Gilbert, Wisconsin Department of Natural Resources). It is therefore highly likely that the genetic similarity of these four populations is due to stocking. Several of the sampled populations from Minnesota also had poorly documented stocking histories yet they remained highly distinct. Genetic structure in Minnesota may have been less eroded if local, genetically similar sources were used, stocking was into larger, healthier resident populations, or stocking was less intense or ended a longer time ago.

Despite the challenges posed by low F_{ST} and evidence of supplemental stocking altering genetic structure in some populations, the SNPs discovered here provide greatly increased resolution for defining reporting units across the midwestern USA. Additionally, simulations suggested that a panel of several hundred loci would be highly capable of conducting individual-based GSI for most genetic units in the region. Given the regional complexity, however, improvements to accuracy could be made by further sampling areas that have shown heterogeneous signals of genetic structure (e.g., due to stocking). For example, increased sampling effort directed at the Chippewa and Wisconsin Rivers' drainage basins could prove especially beneficial as analyzing populations in the lower reaches of each basin may provide a better understanding of signals of historic recolonization, while populations in the upper reaches (e.g., CTWI) could better define the effects stocking may have had. Additional samples could also serve as a holdout dataset, as suggested by Anderson (2010), to test the assignment accuracy of our panel.

Tradeoffs associated with choosing loci based on differentiation versus diversity

We evaluated the tradeoffs associated with selecting SNPs based on differentiation or diversity and found that there was relatively little variation in GSI accuracies across panels. Markers selected based on differentiation have been shown to provide increased resolution for defining reporting groups in systems with low levels of genetic structure (Larson et al., 2014; McKinney et al., 2019). This approach has not, however, been applied to systems where stocking may be a major factor for reduced levels of population structure, such as in Upper Midwestern, USA, walleye. Interestingly, we found that assignment accuracy with our smaller panels was relatively similar to accuracy using 5,000 loci discovered with RAD-seq, the maximum number of loci that rubias was able to process (average difference in assignment accuracy = 1.6%, Fig.

S1). This suggests that assignment accuracy in our system may be limited more by biological realities associated with human-mediated gene flow than by the power of our genetic markers. Further increases in assignment accuracy are therefore likely to be realized through sampling of additional populations and a more refined understanding of population history as opposed to genotyping additional markers.

Conversely, we found that false-positive rates for assigning kin relationships were highly variable among panels, with the microhaplotype diversity-based panel displaying the lowest false-positive rates by several orders of magnitude for each kin relationship (Table 3). Previous work has shown that a false-positive rate of 2.7×10^{-9} at a false-negative rate of 0.015 is capable of conducting parent-offspring assignment in complex marine ecosystems (Baetscher et al., 2019). As such, while loss of the loci through panel optimization was reflected in increased false-positive error rates for the fully optimized panel (Fig. S1), we are confident that final panel retains the power necessary to perform this task in future studies.

The contrast in inter-panel variation between GSI and kinship simulations is reflective of the variation in information content of each panel (Fig. S2), and supports previous findings that while microhaplotype information provided added benefit to both applications, the greatest increase in assignment accuracy will likely be for kinship analysis (Baetscher et al., 2018; McKinney, Seeb, et al., 2017). When attempting to target microhaplotype loci via GT-seq, attention should be given to the number of SNPs one aims to genotype within a locus, as attempting to include loci with too many SNPs may result in targeting repetitive regions that fail to amplify properly in a multiplex. The expected maximum number of alleles per locus and the degree to which loci with large numbers of alleles perturbs primer design will likely vary among taxa. We choose a cutoff of 10 alleles per locus as this appeared to be a natural break point in the allele distribution for walleye; we suggest that researchers investigate this in their system and come up with a logical cutoff prior to selecting loci.

Optimizing primer design and removing overamplifying loci

The main objective of GT-seq primer development is to produce a single pool of primer pairs that will amplify uniformly, while retaining as many loci as possible. To achieve this, it is important to minimize heterogeneity of primer and product characteristics (e.g., primer size, product size) and to understand that the highly multiplexed PCR required by GT-seq can be complicated by hairpin- and inter-primer hybridization artifacts. To best control PCR artifacts, it is important to avoid developing primers with complimentary regions (e.g., complimentary 3' regions and self-complementarity) and apply conservative thresholds to the upper Tm of primer design parameters (Rychlik, 1993). Incorporating loci with multiple SNPs can lead to further difficulties when the ideal priming region also contains a SNP. We found that, while degenerate primers could be successfully amplified in a multiplex, they were culled during optimization at a higher rate than non-degenerate primers. Further performance benefits could be gained from examining DNA template quality beyond just the availability of priming regions, as shown by (Benita et al., 2003) who found regionalized GC content of template DNA to be a predictor of PCR success. This was supported by our data, as loci removed from the panel during optimization displayed significantly higher GC content in the amplicon and primer. Finally, while GT-seq primers can theoretically be designed for a range of amplicon sizes, we suggest that researchers design panels targeting similarly sized products that can be sequenced using PE150 technology. Panels containing similarly sized and relatively short amplicons should reduce variation in amplification rates (Baetscher et al., 2018) and ensure that genotyping is robust to variation in sample quality. Moreover, PE150 sequencing is common to benchtop and core facility sequencing platforms, such as Illumina® MiSeq and HiSeq.

In exploring the upper limits of how many loci a GT-seq panel can target, we found that the number of amplicons reliably genotyped in a single pool is highly dependent on variable rates of amplification among primer pairs during PCR and, to a lesser extent, the degree of primer specificity. Despite efforts to limit primer inter-hybridization through diligent primer design, the presence of overamplifying loci is likely inevitable during early phases of panel development. We found it best to focus primarily on the uniformity of amplification within the primer pool in early optimization steps, by removing primer pairs found to overamplify. Although achieving perfect uniformity is challenging, application of strict cutoffs during initial optimization steps likely results in a final panel that is less influenced by overamplification. The importance of this was illustrated by prop_reads_T10 reducing from 85.0% of all primer reads to 36.6% after optimization. In contrast, loci that displayed low rates of amplification posed little problem and can produce functional sequencing yields after elimination of overamplifiers (data not shown). Likewise, on-target rates were greatly improved by addressing overamplification, as demonstrated by the on-target proportion of reads increasing from 24.9% to 91.7% by the third test.

Further optimization of the GT-seq protocol

Although there may be an upper as-yet-unidentified limit in the number of primers that can be included in a single primer pool, we found that the total number of loci targeted can be increased by PCR amplifying multiple primer pools separately on a sample and pooling PCR products within individuals prior to barcoding. This approach could be used to genotype multiple complementary or even independent GT-seq panels using the same primer tail systems at a small cost increase compared to genotyping a single panel, as the most expensive steps in the GT-seq protocol (e.g., DNA normalization) are only conducted once (Campbell et al., 2015). Combining multiple panels could facilitate genotyping of > 1,000 loci rather than a few hundred, providing greatly increased power for kinship analysis and GSI (Baetscher et al., 2018; McKinney, Seeb, et al., 2017). Additionally, further optimization of individual panels could be conducted by manipulating the initial concentrations of primer pairs based on observed panel performance, reducing the concentration of loci that appear to overamplify. While this process would be cumbersome to perform by hand, a liquid handling robot could enable a researcher to fine-tune the performance of existing and new panels alike, thereby enhancing efficiency.

DNA extraction can comprise a large portion of the total cost of genetic analysis, especially for relatively affordable approaches such as GT-seq, in terms of finances and time. Extractions using chelating beads provided a cost-effective alternative to more expensive salting-out approaches, such as Qiagen DNeasy kits. Chelating extractions, however, can also produce lower quality DNA and may include suspended impurities (Singh et al., 2018). Campbell et al. (2015) did show that GT-seq can be conducted using DNA from chelating extractions but did not directly compare results using multiple extraction protocols. Here, we directly showed that cost-effective chelating extractions can produce equally high quality, if not superior, sequence data compared to more expensive methods. Although consideration should be given to the quality of tissue samples, the chelating approach appears to be a viable approach for reducing per-sample costs with GT-seq. It is important to be aware that proper lab technique is essential when using this method, however, as chelating beads will inhibit PCR and greatly reduce library product yields. This may be especially problematic when using a liquid handling robot that is unable to visually detect chelating beads. Therefore, we suggest researchers carefully pipette the DNA-containing supernatant from chelating resin extractions by hand into a secondary container (e.g., 96-well PCR plate) before aliquoting DNA with a robot. Finally, we found that the ExoSAP procedure included in the original GT-seq protocol did not produce higher quality data and was not necessary for our purposes; removing this step from the protocol will further reduce GT-seq costs and time commitment.

Suggestions for designing GT-seq studies and conclusions

A major consideration when designing a GT-seq panel is deciding how large of an ascertainment dataset is necessary. We constructed a comprehensive ascertainment set with RAD-seq, which was expensive and resource intensive. Despite this, we found that the panel chosen based on diversity produced similar results to the panel chosen based on differentiation. In our case, we believe that a smaller ascertainment set of ~96 individuals sampled from across the same geographic range may have resulted in a panel of relatively similar quality. Smaller ascertainment datasets are likely sufficient when the main applications of a given GT-seq panel are kinship analysis and GSI of highly diverged populations; however, when designing GT-seq panels to differentiate closely related populations (e.g. Chinook salmon *Oncorhynchus tshawytscha* in western Alaska), accurate characterization of ascertainment populations is vital (Larson et al., 2014; McKinney et al., 2019).

Another major consideration when conducting GT-seq analysis is deciding how deep to sequence individuals. We found that a read depth of 31× could be expected to produce genotypes that were 99% concordant with those derived from RADseq. Read depths were, however, highly variable across loci; we only retained 303 of the 436 loci in our panel when we genotyped 536 individuals at an average depth of 33×. We also found that a large and variable proportion of reads can be discarded prior to genotyping. Therefore, we suggest that researchers target an average depth of at least 100× to ensure that most loci in the panel can be genotyped and that all acquired genotypes are highly reliable. At this level of coverage, researchers could genotype ~500 individuals with a panel of 500 loci on a single MiSeq lane (~25 million reads) and ~8,000 individuals on a HiSeq lane (~400 million reads). It is possible this level of coverage is not necessary for some applications, such as GSI, but we strongly suggest obtaining high coverage for more sensitive applications that require high genotyping accuracy, such as kinship analysis.

Finally, researchers conducting GT-seq must consider trade-offs associated with different genotyping approaches. The two main approaches we are aware of are: (1) in-silico probe-based methods that use pattern matching to genotype specific alleles (Campbell et al., 2015; McKinney et al., 2019) and (2) alignment-based methods that call all polymorphisms in a given amplicon (Baetscher et al., 2019). A major advantage of probe-based methods is that databases of probes can be shared among laboratories, facilitating standardization. It is difficult, however, to discover new variation with these methods, whereas alignment-based methods discover new variation by default. We suggest a hybrid approach, where researchers periodically use alignment-based approaches to discover new variation and add this variation to a probe database that forms the basis of genotyping and standardizing genotyping among laboratories.

Genotype-in-thousands sequencing is a powerful addition to the molecular ecologist's toolkit that facilitates rapid, accurate, and cost-effective genetic analysis. Yet, creating a GT-seq panel is non-trivial, and there are many considerations for maximizing the utility of this approach. We found that the greatest challenge when designing our GT-seq panel was locus-specific overamplification, and we suggest that researchers remove these loci liberally. We also found that chelating extractions without an ExoSAP step produce high-quality results, providing a lower-cost alternative to salting-out extractions. Additionally, we showed that combining multiplex PCR products from multiple panels prior to barcoding can ensure additional, potentially important, loci can be genotyped with only a moderate cost increase. Finally, we found that a relatively substantial proportion of sequencing reads are lost before genotyping, and we suggest researchers target higher sequencing coverage (100×) than may apparently be necessary to ensure that GT-seq datasets are robust across loci.

While GT-seq has, to date, been most often applied in fish, many of the over 150 citations of Campbell et al. (2015) at the time of this writing are from perspective papers that discuss the potential of this approach in other taxa. This potential is starting to be realized in non-fish species such as snakes (Schmidt et al. 2019) and aquatic invertebrates (Pavinato et al. 2019), indicating that the GT-seq approach promises to be a mainstay of population genetics for the foreseeable future. The guidelines and suggestions outlined here will hopefully facilitate the spread and effective use of the GT-seq method in a broad array of taxa, allowing researchers to tackle topics that may have been difficult or impossible to address with previous methods.

Acknowledgements

We thank field crews from the Wisconsin and Minnesota Departments of Natural Resources for collecting tissue samples. We also thank Keith Turnquist from UW-Stevens Point for assistance with laboratory analysis and Ana Ramón-Laca for advice regarding primer development. This study was funded by the United States Fish and Wildlife Service, Federal Aid in Sportfish Restoration program and the Wisconsin Department of Natural Resources. Any use of trade, product, or company name is for descriptive purposes only and does not imply endorsement by the U.S. Government.

References

Ackerman, M. W., Habicht, C., & Seeb, L. W. (2011). Single-Nucleotide Polymorphisms (SNPs) under Diversifying Selection Provide Increased Accuracy and Precision in Mixed-Stock

Analyses of Sockeye Salmon from the Copper River, Alaska. *Transactions of the American Fisheries Society, 140*(3), 865-881. doi:10.1080/00028487.2011.588137

Ackiss, A. S., Larson, W. A., & Stott, W. (2020). Genotyping-by-sequencing illuminates high levels of divergence among sympatric forms of coregonines in the Laurentian Great Lakes. *Evolutionary Applications, n/a*(n/a). doi:10.1111/eva.12919

Ali, O. A., O'Rourke, S. M., Amish, S. J., Meek, M. H., Luikart, G., Jeffres, C., & Miller, M. R. (2016). RAD Capture (Rapture): Flexible and Efficient Sequence-Based Genotyping. *Genetics, 202*(2), 389-400. doi:10.1534/genetics.115.183665

Anderson, E. C. (2010). Assessing the power of informative subsets of loci for population assignment: standard methods are upwardly biased. *Molecular Ecology Resources, 10*(4), 701-710. doi:10.1111/j.1755-0998.2010.02846.x

Anderson, E. C., & Garza, J. C. (2006). The power of single-nucleotide polymorphisms for large-scale parentage inference. *Genetics, 172*(4), 2567-2582. doi:10.1534/genetics.105.048074

Baetscher, D. S., Anderson, E. C., Gilbert-Horvath, E. A., Malone, D. P., Saarman, E. T., Carr, M. H., & Garza, J. C. (2019). Dispersal of a nearshore marine fish connects marine reserves and adjacent fished areas along an open coast. *Molecular Ecology, 28*(7), 1611-1623. doi:10.1111/mec.15044

Baetscher, D. S., Clemento, A. J., Ng, T. C., Anderson, E. C., & Garza, J. C. (2018). Microhaplotypes provide increased power from short-read DNA sequences for relationship inference. *Mol Ecol Resour, 18*(2), 296-305. doi:10.1111/1755-0998.12737

Bay, R. A., Taylor, E. B., & Schluter, D. (2019). Parallel introgression and selection on introduced alleles in a native species. *Molecular Ecology, 28*(11), 2802-2813. doi:10.1111/mec.15097

Benita, Y., Oosting, R. S., Lok, M. C., Wise, M. J., & Humphery‐Smith, I. (2003). Regionalized GC content of template DNA as a predictor of PCR success. *Nucleic Acids Research, 31*(16), e99-e99. doi:10.1093/nar/gng101

Bradbury, I. R., Hubert, S., Higgins, B., Sharen, B., Paterson, I. G., Snelgrove, P. V. R., . . . Bentzen, P. (2011). Evaluating SNP ascertainment bias and its impact on population assignment in Atlantic cod, Gadus morhua. *Molecular Ecology Resources, 11*(s1), 218-225. doi:10.1111/j.1755-0998.2010.02949.x

Brumfield, R. T., Beerli, P., Nickerson, D. A., & Edwards, S. V. (2003). The utility of single nucleotide polymorphisms in inferences of population history. *Trends in Ecology & Evolution, 18*(5), 249-256. doi:https://doi.org/10.1016/S0169-5347(03)00018-1

Campbell, N. R., Harmon, S. A., & Narum, S. R. (2015). Genotyping-in-Thousands by sequencing (GT-seq): A cost effective SNP genotyping method based on custom amplicon sequencing. *Molecular Ecology Resources, 15*(4), 855-867. doi:10.1111/1755-0998.12357

Chen, K., Zhou, Y.-x., Li, K., Qi, L.-x., Zhang, Q.-f., Wang, M.-c., & Xiao, J.-h. (2016). A novel three-round multiplex PCR for SNP genotyping with next generation sequencing. *Analytical and Bioanalytical Chemistry, 408*(16), 4371-4377. doi:10.1007/s00216-016-9536-6

Danecek, P., Auton, A., Abecasis, G., Albers, C. A., Banks, E., DePristo, M. A., . . . Group, G. P. A. (2011). The variant call format and VCFtools. *Bioinformatics, 27*(15), 2156-2158. doi:10.1093/bioinformatics/btr330

Davey, J. W., Hohenlohe, P. A., Etter, P. D., Boone, J. Q., Catchen, J. M., & Blaxter, M. L. (2011). Genome-wide genetic marker discovery and genotyping using next-generation sequencing. *Nature Reviews Genetics, 12*(7), 499-510. doi:10.1038/nrg3012

Embke, H. S., Rypel, A. L., Carpenter, S. R., Sass, G. G., Ogle, D., Cichosz, T., . . . Vander Zanden, M. J. (2019). Production dynamics reveal hidden overharvest of inland recreational fisheries. *Proceedings of the National Academy of Sciences, 116*(49), 24676. doi:10.1073/pnas.1913196116

Euclide, P. T., McKinney, G. J., Bootsma, M., Tarsa, C., Meek, M. H., & Larson, W. A. (2020). Attack of the PCR clones: Rates of clonality have little effect on RAD-seq genotype calls. *Molecular Ecology Resources, 20*(1), 66-78. doi:10.1111/1755-0998.13087

Garza, J. C., & Freimer, N. B. (1996). Homoplasy for size at microsatellite loci in humans and chimpanzees. *Genome Research, 6*(3), 211-217. doi:10.1101/gr.6.3.211

Hammen, J. J., & Sloss, B. L. (2019). Walleye Genetic Characterization in the Northern Ceded Territory of Wisconsin: Implications for Stocking Using Conservation Strategies. *North American Journal of Fisheries Management, 0*(0). doi:10.1002/nafm.10302

Hanken, J., & Sherman, P. W. (1981). Multiple Paternity in Belding's Ground Squirrel Litters. *Science, 212*(4492), 351-353.

Hansen, J., Sass, G., Gaeta, J., Hansen, G., Isermann, D., Lyons, J., . . . Carpenter, S. (2015). Largemouth Bass Management in Wisconsin: Intra- and Inter-Specific Implications of Abundance Increases.

Hoffman, J. I., Simpson, F., David, P., Rijks, J. M., Kuiken, T., Thorne, M. A. S., . . . Dasmahapatra, K. K. (2014). High-throughput sequencing reveals inbreeding depression in a natural population. *Proceedings of the National Academy of Sciences, 111*(10), 3775. doi:10.1073/pnas.1318945111

Jombart, T., & Ahmed, I. (2011). adegenet 1.3-1: new tools for the analysis of genome-wide SNP data. *Bioinformatics, 27*(21), 3070-3071. doi:10.1093/bioinformatics/btr521

Keenan, K., McGinnity, P., Cross, T. F., Crozier, W. W., & Prodöhl, P. A. (2013). diveRsity: An R package for the estimation and exploration of population genetics parameters and their associated errors. *Methods in Ecology and Evolution, 4*(8), 782-788. doi:10.1111/2041-210X.12067

Larson, W. A., Seeb, J. E., Pascal, C. E., Templin, W. D., Seeb, L. W., & Taylor, E. (2014). Single-nucleotide polymorphisms (SNPs) identified through genotyping-by-sequencing improve genetic stock identification of Chinook salmon (Oncorhynchus tshawytscha) from western Alaska. *Canadian Journal of Fisheries & Aquatic Sciences, 71*(5), 698-708. doi:10.1139/cjfas-2013-0502

Logsdon, D. E., Anderson, C. S., & Miller, L. M. (2016). Contribution and Performance of Stocked Walleyes in the Recovery of the Red Lakes, Minnesota, Fishery. *North American Journal of Fisheries Management, 36*(4), 828-843. doi:10.1080/02755947.2016.1167143

Luikart, G., & England, P. R. (1999). Statistical analysis of microsatellite DNA data. *Trends in Ecology & Evolution, 14*(7), 253-256. doi:10.1016/S0169-5347(99)01632-8

McKinney, G. J., Pascal, C. E., Templin, W. D., Gilk-Baumer, S. E., Dann, T. H., Seeb, L. W., & Seeb, J. E. (2019). Dense SNP panels resolve closely related Chinook salmon populations. *Canadian Journal of Fisheries and Aquatic Sciences*. doi:10.1139/cjfas-2019-0067

McKinney, G. J., Seeb, J. E., & Seeb, L. W. (2017). Managing mixed-stock fisheries: genotyping multi-SNP haplotypes increases power for genetic stock identification. *Canadian Journal of Fisheries and Aquatic Sciences, 74*(4), 429-434. doi:10.1139/cjfas-2016-0443

McKinney, G. J., Waples, R. K., Pascal, C. E., Seeb, L. W., & Seeb, J. E. (2018). Resolving allele dosage in duplicated loci using genotyping-by-sequencing data: A path forward for population genetic analysis. *Molecular Ecology Resources, 18*(3), 570-579. doi:10.1111/1755-0998.12763

McKinney, G. J., Waples, R. K., Seeb, L. W., & Seeb, J. E. (2017). Paralogs are revealed by proportion of heterozygotes and deviations in read ratios in genotyping-by-sequencing data from natural populations. *Mol Ecol Resour, 17*(4), 656-669. doi:10.1111/1755-0998.12613

Meek, M. H., & Larson, W. A. (2019). The future is now: Amplicon sequencing and sequence capture usher in the conservation genomics era. *Molecular Ecology Resources, 19*(4), 795-803. doi:10.1111/1755-0998.12998

Milner, G., Teel, D. J., Utter, F. M., & Winans, G. A. (1985). A genetic method of stock identification in mixed populations of Pacific salmon, Oncorynchus spp. *Marine Fisheries Review, 47*, 1.

Moran, B. M., & Anderson, E. C. (2018). Bayesian inference from the conditional genetic stock identification model. *Canadian Journal of Fisheries & Aquatic Sciences, 76*(4), 551-560. doi:10.1139/cjfas-2018-0016

Morin, P. A., Luikart, G., Wayne, R. K., & the, S. N. P. w. g. (2004). SNPs in ecology, evolution and conservation. *Trends in Ecology & Evolution, 19*(4), 208-216. doi:https://doi.org/10.1016/j.tree.2004.01.009

Narum, S. R., Buerkle, C. A., Davey, J. W., Miller, M. R., & Hohenlohe, P. A. (2013). Genotyping-by-sequencing in ecological and conservation genomics. *Mol Ecol, 22*(11), 2841-2847. doi:10.1111/mec.12350

Natesh, M., Taylor, R. W., Truelove, N. K., Hadly, E. A., Palumbi, S. R., Petrov, D. A., & Ramakrishnan, U. (2019). Empowering conservation practice with efficient and economical genotyping from poor quality samples. *Methods in Ecology and Evolution, 10*(6), 853-859. doi:10.1111/2041-210X.13173

Navajas, M. J., Thistlewood, H. M. A., Lagnel, J., & Hughes, C. (1998). Microsatellite sequences are under-represented in two mite genomes. *Insect Molecular Biology, 7*(3), 249-256. doi:10.1111/j.1365-2583.1998.00066.x

Nielsen, R., Paul, J. S., Albrechtsen, A., & Song, Y. S. (2011). Genotype and SNP calling from next-generation sequencing data. *Nature Reviews Genetics, 12*(6), 443-451. doi:10.1038/nrg2986

Onda, Y., Takahagi, K., Shimizu, M., Inoue, K., & Mochida, K. (2018). Multiplex PCR Targeted Amplicon Sequencing (MTA-Seq): Simple, Flexible, and Versatile SNP Genotyping by Highly Multiplexed PCR Amplicon Sequencing. *Frontiers in Plant Science, 9*, 201.

Pavinato, V. A. C., Wijeratne, S., Spacht, D., Denlinger, D. L., Meulia, T., & Michel, A. P. (2019). Leveraging targeted sequencing for non-model species: a step-by-step guide to obtain a reduced SNP set and a pipeline to automate data processing in the Antarctic Midge, &lt;em&gt;Belgica antarctica&lt;/em&gt;. *bioRxiv*, 772384. doi:10.1101/772384

Reid, K., Carlos Garza, J., Gephard, S. R., Caccone, A., Post, D. M., & Palkovacs, E. P. (2019). Restoration-mediated secondary contact leads to introgression of alewife ecotypes separated by a colonial-era dam. *Evolutionary Applications, n/a*(n/a). doi:10.1111/eva.12890

Rochette, N. C., Rivera-Colón, A. G., & Catchen, J. M. (2019). Stacks 2: Analytical methods for paired-end sequencing improve RADseq-based population genomics. *Molecular Ecology, 28*(21), 4737-4754. doi:10.1111/mec.15253

Rychlik, W. (1993). Selection of Primers for Polymerase Chain Reaction. In B. A. White (Ed.), *PCR Protocols: Current Methods and Applications* (pp. 31-40). Totowa, NJ: Humana Press.

Rypel, A. L., Goto, D., Sass, G. G., & Zanden, M. J. V. (2018). Eroding productivity of walleye populations in northern Wisconsin lakes. *Canadian Journal of Fisheries and Aquatic Sciences, 75*, 2291+.

Schmidt, D., Campbell, N. R., Govindarajulu, P., Larsen, K. W., & Russello, M. A. (2019). Genotyping-in-Thousands by sequencing (GT-seq) panel development and application to minimally-invasive DNA samples to support studies in molecular ecology. *Molecular Ecology Resources, 0*(ja). doi:10.1111/1755-0998.13090

Seeb, J. E., Carvalho, G., Hauser, L., Naish, K., Roberts, S., & Seeb, L. W. (2011). Single-nucleotide polymorphism (SNP) discovery and applications of SNP genotyping in nonmodel organisms. *Molecular Ecology Resources, 11*, 1-8. doi:10.1111/j.1755-0998.2010.02979.x

Singh, U. A., Kumari, M., & Iyengar, S. (2018). Method for improving the quality of genomic DNA obtained from minute quantities of tissue and blood samples using Chelex 100 resin. *Biological Procedures Online, 20*.

Smith, C. T., Antonovich, A., Templin, W. D., Elfstrom, C. M., Narum, S. R., & Seeb, L. W. (2007). Impacts of Marker Class Bias Relative to Locus-Specific Variability on Population Inferences in Chinook Salmon: A Comparison of Single-Nucleotide Polymorphisms with Short Tandem Repeats and Allozymes. *Transactions of the American Fisheries Society, 136*(6), 1674-1687. doi:10.1577/T06-227.1

Stepien, C., A., Murphy, D., J., Lohner, R., N., Sepulveda‐Villet O, J., & Haponski, A., E. (2009). Signatures of vicariance, postglacial dispersal and spawning philopatry: population genetics of the walleye Sander vitreus. *Molecular Ecology, 18*(16), 3411-3428. doi:10.1111/j.1365-294X.2009.04291.x

Storer, C. G., Pascal, C. E., Roberts, S. B., Templin, W. D., Seeb, L. W., & Seeb, J. E. (2012). Rank and Order: Evaluating the Performance of SNPs for Individual Assignment in a Non-Model Organism. *PLOS ONE, 7*(11), 1-13. doi:10.1371/journal.pone.0049018

Untergasser, A., Cutcutache, I., Koressaar, T., Ye, J., Faircloth, B. C., Remm, M., & Rozen, S. G. (2012). Primer3--new capabilities and interfaces. *Nucleic Acids Research, 40*(15), e115-e115. doi:10.1093/nar/gks596

Wagner, C. E., Keller, I., Wittwer, S., Selz, O. M., Mwaiko, S., Greuter, L., . . . Seehausen, O. (2013). Genome-wide RAD sequence data provide unprecedented resolution of species boundaries and relationships in the Lake Victoria cichlid adaptive radiation. *Molecular Ecology, 22*(3), 787-798. doi:10.1111/mec.12023

Westbrook, L. J. (2012). *Genetic structure of rock bass and johnny darters: Implications for gamefish management in Wisconsin.* (Master's), University of Wisconsin, Stevens Point,

Willi, Y., van Kleunen, M., Dietrich, S., & Fischer, M. (2007). Genetic rescue persists beyond first-generation outbreeding in small populations of a rare plant. *Proceedings of the Royal Society B: Biological Sciences, 274*(1623), 2357-2364. doi:10.1098/rspb.2007.0768

Data accessibility

Raw data for the RADseq and GT-seq data obtained in this study was deposited to the NCBI sequence read archive (SUB####) and VCF files of genotypes are available on DRYAD (DOI: PENDING). Python and R scripts used in the statistical analysis pipeline are available at GIT

Author contributions

WL, GS, KG, and LM designed the study with input from MB. Data analyses were conducted by MB with assistance from GM. Laboratory analysis was conducted by MB, KG, and LS. All authors contributed to the writing of the manuscript.

Tables

Table 1. Information on walleye collections from 23 sites in Wisconsin and Minnesota. Reporting units are aggregations of genetically similar populations grouped for GSI analysis, n sampled is the number of individuals that were RAD sequenced, n past filters is the number of individuals missing genotypes at < 30% of SNPs and retained after quality filtering. Diversity statistics calculated using 20,579 SNPs. The F_{ST_600}, Composite$_{\_600,}$ and Diversity$_{\_600}$ columns are the percent correct assignment to reporting group for each population with 100% simulations conducted using the corresponding panel.

Population ID	Reporting Unit	Population	Latitude	Longitude	n sampled	n past filters	H_E	H_O	F_{IS}	AR	F_{ST_600}	Composite$_{\_600}$	Diversity $_{600}$
1	Rock-Fox	Delavan Lake	42.58	-88.63	48	48	0.169	0.168	0.008	1.607	1.00	1.00	1.00
2	Wolf River	Lake Winnebago	44.36	-88.69	47	41	0.173	0.186	-0.05	1.645	1.00	1.00	1.00
3	Upper Wisconsin	Lake Wisconsin	43.38	-89.58	48	45	0.179	0.175	0.017	1.674	1.00	1.00	1.00
4	Upper Wisconsin	Medicine Lake Chain	45.81	-89.13	47	47	0.166	0.166	0.004	1.604	0.96	0.98	0.98
5	Upper Wisconsin	Willow Flowage	45.71	-89.87	48	48	0.176	0.174	0.013	1.657	1.00	1.00	0.99
6	Upper Wisconsin	Kawaguesaga Lake	45.86	-89.74	48	42	0.17	0.167	0.013	1.638	0.96	0.94	0.94
7	Upper Wisconsin	Big Arbor Vitae Lake	45.93	-89.65	48	44	0.174	0.174	0.005	1.654	0.74	0.96	0.99
8	Upper Chippewa	Escanaba Lake	46.06	-89.59	48	44	0.168	0.173	-0.018	1.623	NA	NA	NA
9	Upper Chippewa	Sanford Lake	46.18	-89.69	48	44	0.157	0.164	-0.033	1.528	NA	NA	NA
10	Upper Chippewa	Manitowish Lake	46.11	-89.85	47	35	0.172	0.175	-0.006	1.647	0.58	0.57	0.51
11	Upper Chippewa	Turtle Flambeau Flowage	46.06	-90.13	47	38	0.173	0.172	0.005	1.661	0.63	0.55	0.76
12	Upper Chippewa	Chippewa Flowage	45.90	-91.09	47	43	0.173	0.175	-0.006	1.658	0.88	0.89	0.93
13	Upper Chippewa	Eau Claire River	44.80	-91.50	47	47	0.161	0.162	-0.001	1.583	0.98	0.98	0.98
14	Upper Chippewa	Lake Millicent	46.53	-91.37	48	32	0.167	0.176	-0.034	1.623	NA	NA	NA
15	Lake Superior	St. Louis River	46.65	-92.21	32	30	0.17	0.168	0.006	1.621	0.77	0.77	0.77
16	Vermilion River	Pike River	47.59	-92.39	32	28	0.144	0.142	0.005	1.498	1.00	1.00	1.00
17	Des Moines River	Lake Sarah	44.15	-95.77	32	30	0.164	0.166	-0.006	1.597	1.00	1.00	1.00
18	North Fork Crow River	Lake Koronis	45.33	-94.70	32	17	0.155	0.155	-0.011	1.579	0.82	0.82	0.75
19	Rum River	Mille Lacs Lake	46.25	-93.67	32	29	0.148	0.151	-0.018	1.511	1.00	1.00	1.00
20	Pine River	Pine River	46.70	-94.39	32	30	0.156	0.162	-0.028	1.547	0.97	0.97	0.97
21	Mississippi River - Headwaters	Cutfoot Sioux Lake	47.50	-94.09	32	25	0.147	0.148	-0.011	1.517	1.00	1.00	1.00
22	Otter Tail River	Ottertail Lake	46.41	-95.66	32	23	0.158	0.16	-0.016	1.568	1.00	1.00	0.97
23	Red Lake	Red Lake	47.91	-95.04	32	29	0.149	0.153	-0.025	1.514	0.90	0.86	0.83

Table 2. Summary of pairwise F_{ST} comparisons between walleye *Sander vitreus* populations grouped by state of origin. Abbreviations are Wisconsin (WI) and Minnesota (MN).

	WI-WI	**MN-MN**	**WI-MN**
Max	0.106	0.142	0.142
Mean	0.032	0.068	0.072
Min	0.001	0.019	0.026

Table 3. Summary statistics by SNP panel tested for walleye *Sander vitreus* in Wisconsin and Minnesota, USA, including: average F_{ST}, heterozygosity (H_{E_mhap}), assignment accuracy to population and reporting unit of origin in 100% simulations, and estimated false-positive rates (FPR) for a given kin relationship at a false-negative rate (FNR) of 0.01.

	$F_{ST\ 600}$	**Composite** $_{600}$	**Diversity** $_{600}$
Average F_{ST}	0.117	0.076	0.047
Average H_{E_mhap}	0.389	0.569	0.633
Average accuracy by reporting unit	0.937	0.937	0.929
Average accuracy by population	0.864	0.861	0.862
Parent-offspring FPR (FNR = 0.01)	4.68×10^{-34}	7.92×10^{-62}	2.74×10^{-80}
Full-sibling FPR (FNR = 0.01)	3.42×10^{-29}	5.34×10^{-50}	1.16×10^{-64}
Half-sibling FPR (FNR = 0.01)	6.44×10^{-6}	2.56×10^{-10}	2.06×10^{-13}

Table 4. Summary of GT-seq optimization runs for walleye *Sander vitreus* in Wisconsin and Minnesota, USA. Rows report number of primer pairs targeted, number of reads with intact i-7 barcodes (retained reads), number of retained reads with *in-silico* primer sequences (total reads), number of total reads with *in-silico* probe sequences (on-target reads), percent of total reads on-target, percent of total reads allocated to the 10% of loci tested with highest rank total read counts, average number of SNPs per locus, and average GC content in the forward and reverse primers.

	Test 1	**Test 2**	**Test 3**
Total primer pairs	600	477	436
i7 reads	4,655,071	12,653,262	7,282,101
i7 reads w/ primers	4,150,910	9,347,591	6,827,424
i7 reads w/ primers & probes	1,031,707	3,268,293	6,262,523
On-target percent of total reads	24.9%	35.0%	91.7%
Percent reads in top 10% of loci	85.0%	72.5%	36.6%
mean SNPs per locus	2.06	2.00	1.97
mean GC percent forward primer	51.0%	50.4%	50.3%
mean GC percent reverse primer	49.0%	48.3%	48.2%

Figure captions

Figure 1. Generalized workflow describing major steps inherent in *de novo* construction of a high-density SNP panel for walleye *Sander vitreus* in Wisconsin and Minnesota, USA.

Figure 2. (a) Map of walleye *Sander vitreus* in Wisconsin and Minnesota, USA, collection locations and (b) dendrogram of sampled populations with bootstrap support (n = 1000) estimates above nodes. Branch lengths correspond to genetic distances estimated using Nei's DA. Figures color coded according to major drainage of origin (Hudson Bay: yellow, Mississippi: green, Great Lakes: blue) and numbered with respect to order in Table 1.

Figure 3. (a) Violin plots showing densities of accuracy estimates from 100% simulations of 20 populations of walleye *Sander vitreus* in Wisconsin and Minnesota, USA, performed using 1,000 iterations for each test panel by reporting unit and (b) simulated false-positive rate estimates across a range of false-negative rates. Figures color coded according to SNP panel tested: $F_{\mathrm{ST\_600}}$ (red, 600 rank F_{ST} loci), Composite$_{\_600}$ (black, 300 rank F_{ST} and 300 rank $H_{\mathrm{E\_mhap}}$ loci), and Diversity$_{\_600}$ (purple, 600 rank $H_{\mathrm{E\_mhap}}$ loci).

Figure 4. Relative $\log_{10}$ total read counts per locus (black) and relative $\log_{10}$ on-target read counts per locus (green) of the GT-seq panel for walleye *Sander vitreus* in Wisconsin and Minnesota, USA, prior to optimization (a, 600 loci), after first optimization (b, 477 loci), and after second optimization (c, 436 loci). Loci identified for culling during optimization steps shown in orange and read counts annotated in boxes.

Figure 5. Number of on-target reads (green) and proportion of total reads on-target obtained from GT-seq libraries produced using DNAs extracted via Chelex, Chelex with ExoSAP, and Qiagen with ExoSAP. Significantly different groups denoted by letters on box.

Figure 6. Modeled relationship between GT-seq read depth and genotype concordance between GT-seq and RADseq shown in gray (1.00-0.34/GT-seq read depth, rss = 0.02) with 95% confidence intervals in red. GT-seq read depth at which estimated genotype concordance equals 99% (96.2%-100%) represented by blue line. Black points display proportion of genotypes found identical between GT-seq and RADseq for GT-seq read depth bins with > 30 genotypes.

Figure 7. Variation in read depth among individuals at loci successfully genotyped after quality filtering (303 loci with < 30% missing data). Average read depth at each locus shown with black points, while gray points denote first and third quartile for each locus. Dotted blue line denotes target read depth of 30×. Data from 551 walleye sequenced using fully optimized panel. Average read depth among all loci is 33×.

Supplementary materials

Table S1. Pairwise F_{ST} estimates for all sampled walleye *Sander vitreus* populations (sites numbered according to Table 1 and Fig. 1 A). Estimates produced in arlequin v3.5.2.

Table S2. Summary statistics for 20,597 SNPs retained through initial filtering based on maximum missingness rates of < 30% and HDplot cutoffs of H > 0.5 and -7 < D < 7. Columns include a locus tag (CHROM), position of SNP within locus (Reid et al.), a unique SNP value

(ID), reference (REF) and alternate (Keenan et al.) SNP alleles, global F_{IS} (Willi et al.), single SNP F_{ST} (Smith et al.), expected microhaplotype heterozygosity (mhap_H_E), and number of alleles per locus tag (n_alleles). Diversity statistics estimated in diveRsity v1.9.90 (global F_{IS} and single SNP F_{ST}) and adegenet v2.1.1 (single locus H_E, number of alleles).

Table S3. Summary matrix of 100% simulations (reps = 1,000, mixsize = 200) for each sampled population retained through filtering, performed using the F_{ST_600} panel. Each row represents a simulation for the listed population name. Each column within a row represents the proportion of individuals assigned to the population denoted at the top of the column. Unassigned individuals (< 70% probability of origin from a given population) accounted for in last column.

Table S4. Summary matrix of 100% simulations (reps = 1,000, mixsize = 200) for each sampled population retained through filtering steps, performed using the Composite$_{\_600}$ panel. Each row represents a simulation for the listed population name. Each column within a row represents the proportion of individuals assigned to the population denoted at the top of the column. Unassigned individuals (< 70% probability of origin from a given population) are accounted for in the last column.

Table S5. Summary matrix of 100% simulations (reps = 1,000, mixsize = 200) for each sampled population retained through filtering steps, performed using the Diversity$_{\_600}$ panel. Each row represents a simulation for the listed population name. Each column within a row represents the proportion of individuals assigned to the population denoted at the top of the column. Unassigned individuals (< 70% probability of origin from a given population) are accounted for in the last column.

Figure S1. (a) Violin plots showing densities of accuracy estimates from 100% simulations of 20 populations of walleye Sander vitreus in Wisconsin and Minnesota, USA, performed using 1,000 iterations for each test panel by reporting unit and (b) simulated false-positive rate estimates across a range of false-negative rates. Figures color coded according to SNP panel tested: Final 436 (light blue,the 436 loci retained through all optimization steps), Primed 600 (dark blue, the 600 loci for which primer pairs were successfully designed), and 5,000 loci (brown, 5,000 randomly selected loci).

Figure S2. Frequency distribution of number of alleles among 600 loci tested in each panel.

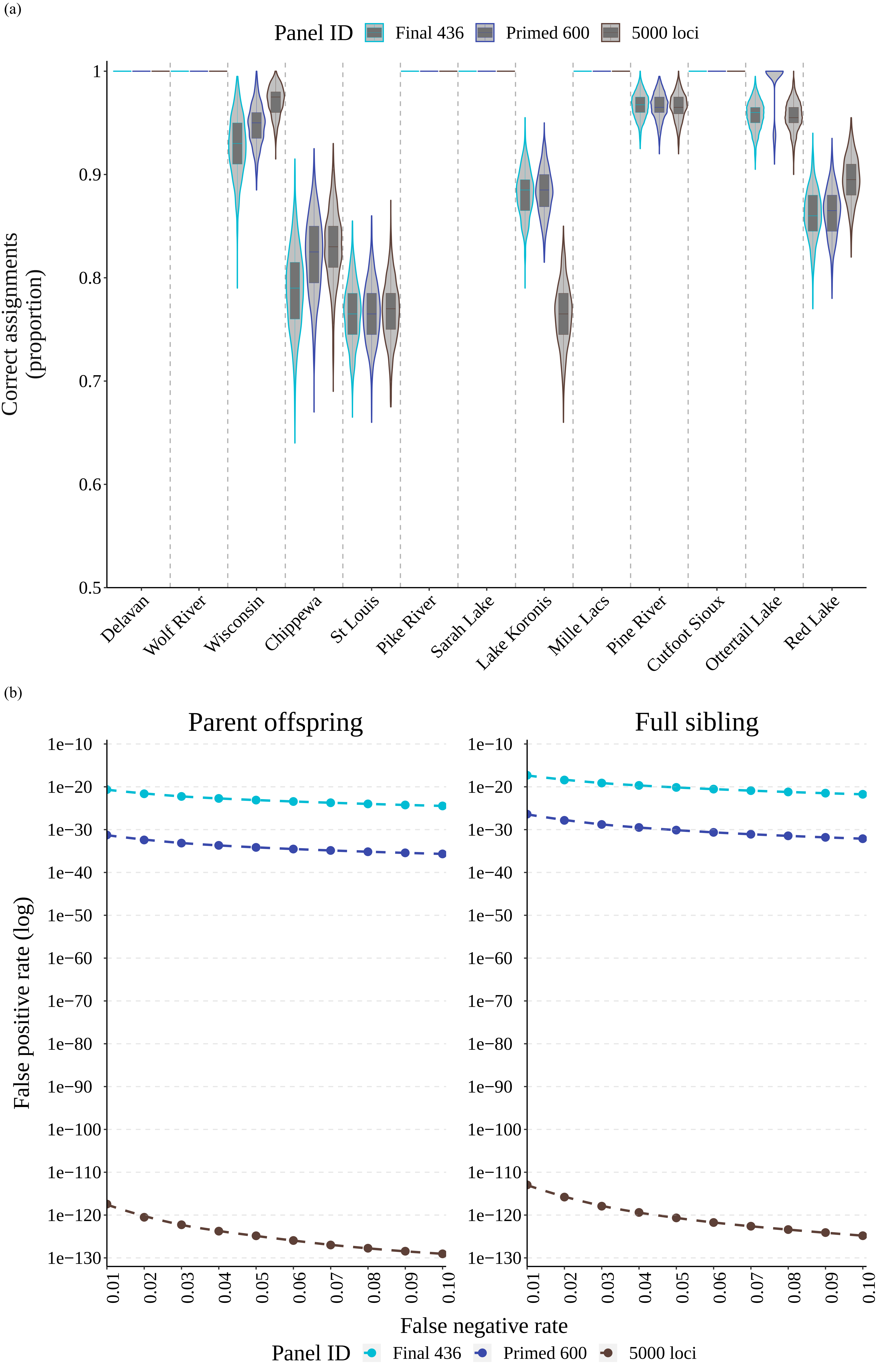
(a)
Panel ID
Final 436
Primed 600
5000 loci
Correct assignments (proportion)
1
0.9
0.8
0.7
0.6
0.5
Delavan
Wolf River
Wisconsin
Chippewa
St Louis
Pike River
Sarah Lake
Lake Koronis
Mille Lacs
Pine River
Cutfoot Sioux
Ottertail Lake
Red Lake
(b)
Parent offspring
Full sibling
False positive rate (log)
1e−10
1e−20
1e−30
1e−40
1e−50
1e−60
1e−70
1e−80
1e−90
1e−100
1e−110
1e−120
1e−130
0.01
0.02
0.03
0.04
0.05
0.06
0.07
0.08
0.09
0.10
False negative rate
Panel ID
Final 436
Primed 600
5000 loci

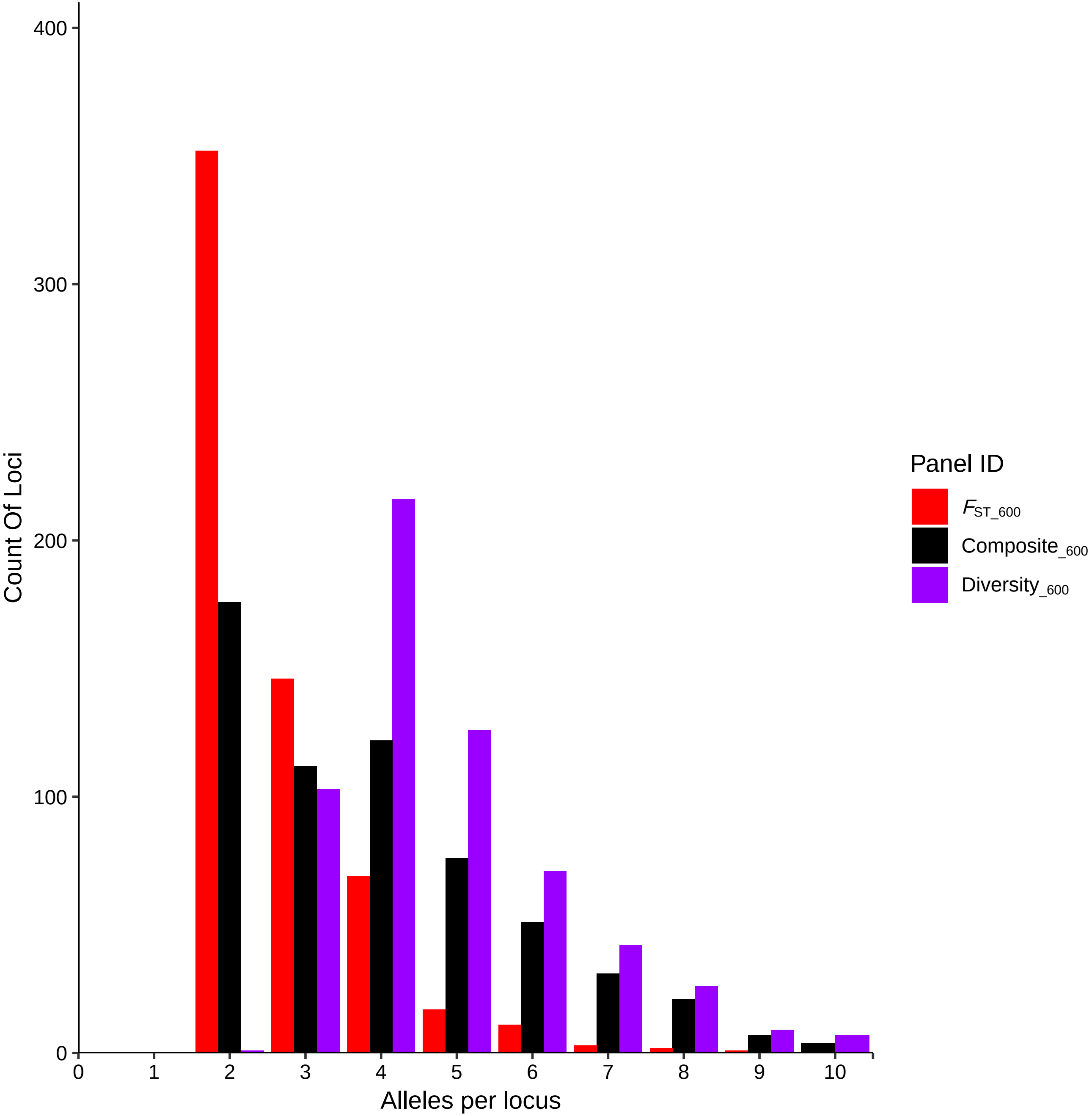
400
300
200
100
0
Count Of Loci
0
1
2
3
4
5
6
7
8
9
10
Alleles per locus
Panel ID
$F_{\mathrm{ST\_600}}$
Composite$_{\_600}$
Diversity$_{\_600}$

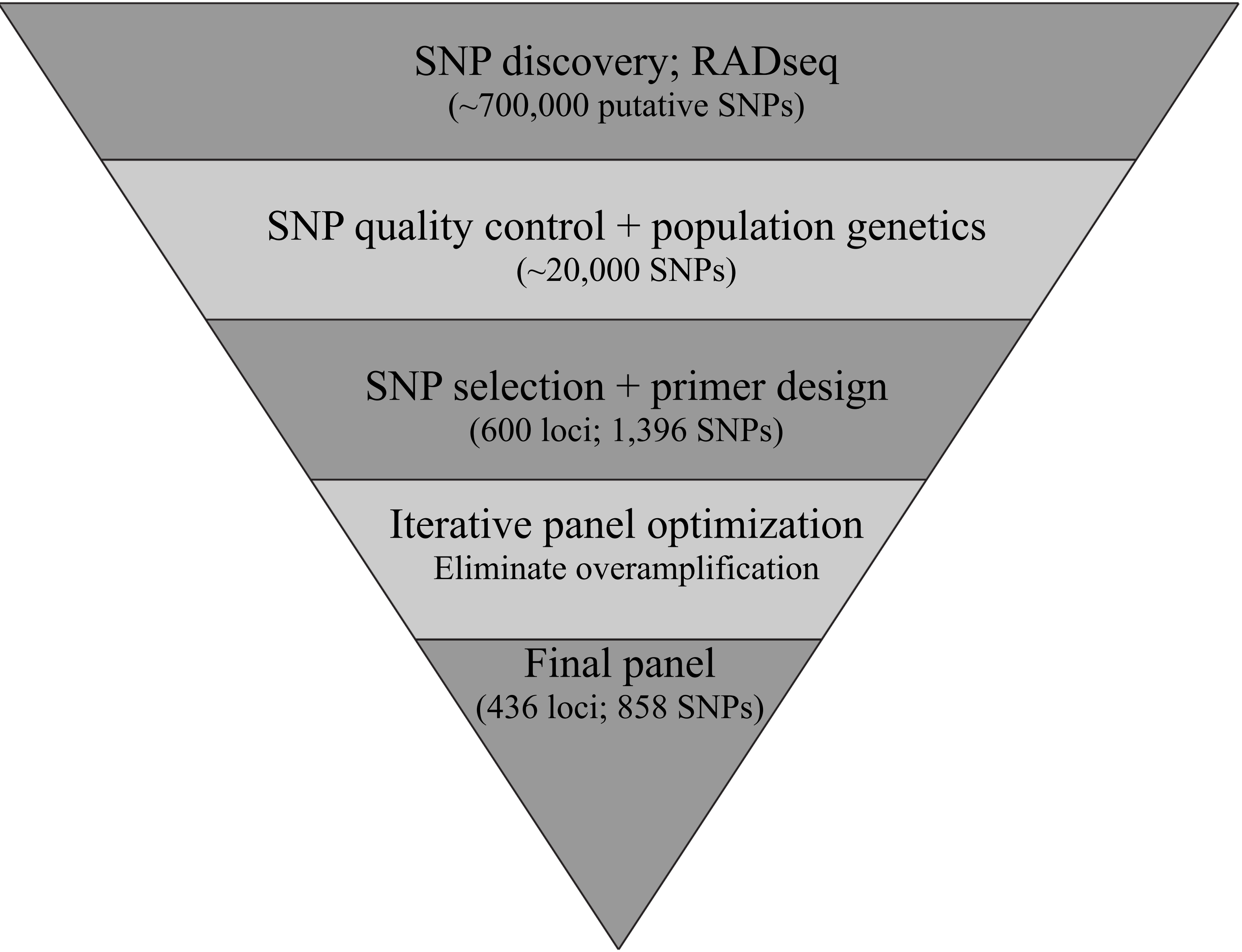
SNP discovery; RADseq
(~700,000 putative SNPs)
SNP quality control + population genetics
(~20,000 SNPs)
SNP selection + primer design
(600 loci; 1,396 SNPs)
Iterative panel optimization
Eliminate overamplification
Final panel
(436 loci; 858 SNPs)

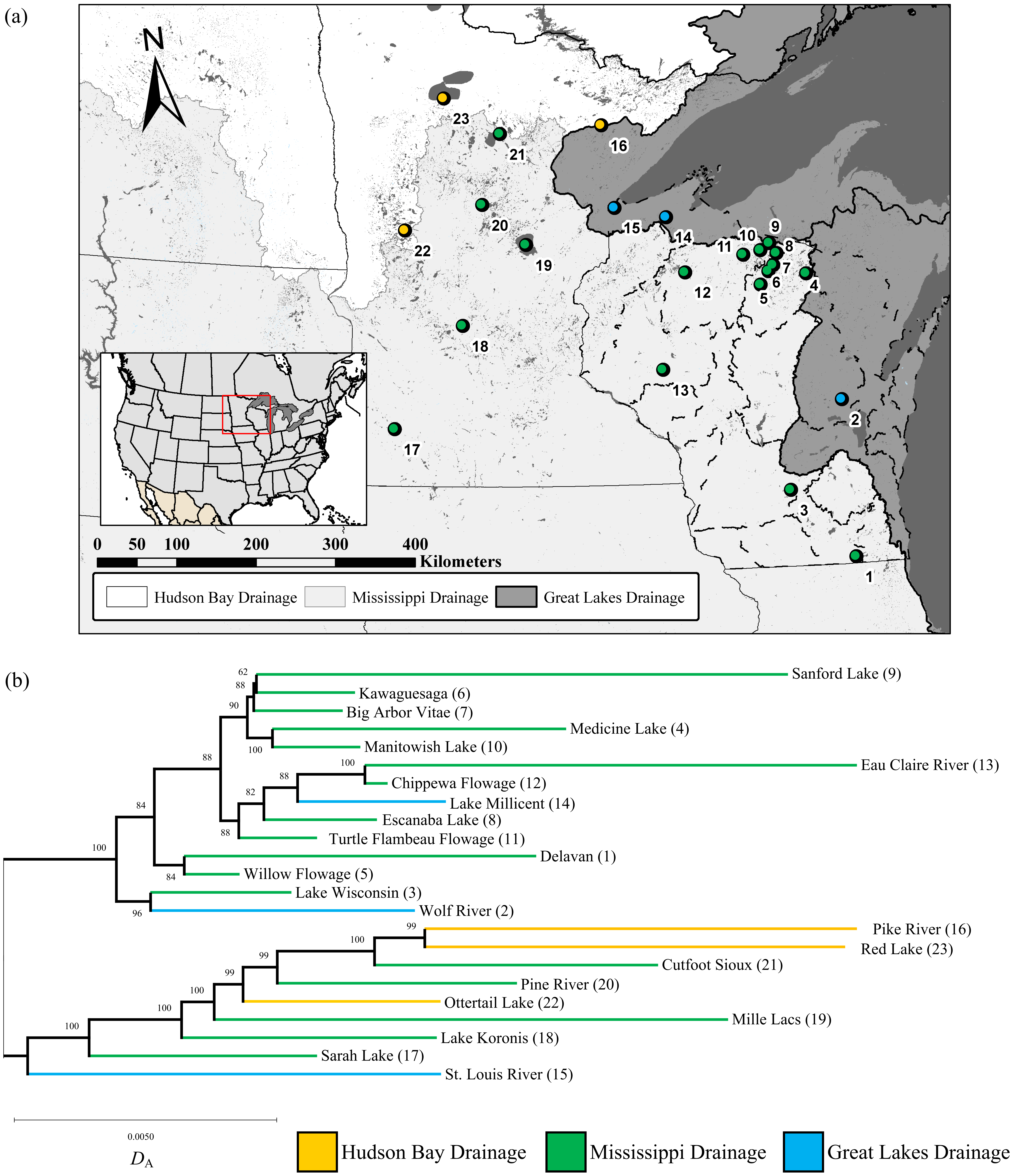
(a)
N
23
21
16
20
22
19
15
14
10
9
11
8
7
4
6
5
12
18
13
2
17
3
1
0
50
100
200
300
400
Kilometers
Hudson Bay Drainage
Mississippi Drainage
Great Lakes Drainage
(b)
62
88
90
100
88
84
100
88
82
88
84
100
96
99
100
99
99
100
100
100
Sanford Lake (9)
Kawaguesaga (6)
Big Arbor Vitae (7)
Medicine Lake (4)
Manitowish Lake (10)
Eau Claire River (13)
Chippewa Flowage (12)
Lake Millicent (14)
Escanaba Lake (8)
Turtle Flambeau Flowage (11)
Delavan (1)
Willow Flowage (5)
Lake Wisconsin (3)
Wolf River (2)
Pike River (16)
Red Lake (23)
Cutfoot Sioux (21)
Pine River (20)
Ottertail Lake (22)
Mille Lacs (19)
Lake Koronis (18)
Sarah Lake (17)
St. Louis River (15)
0.0050
D_A
Hudson Bay Drainage
Mississippi Drainage
Great Lakes Drainage

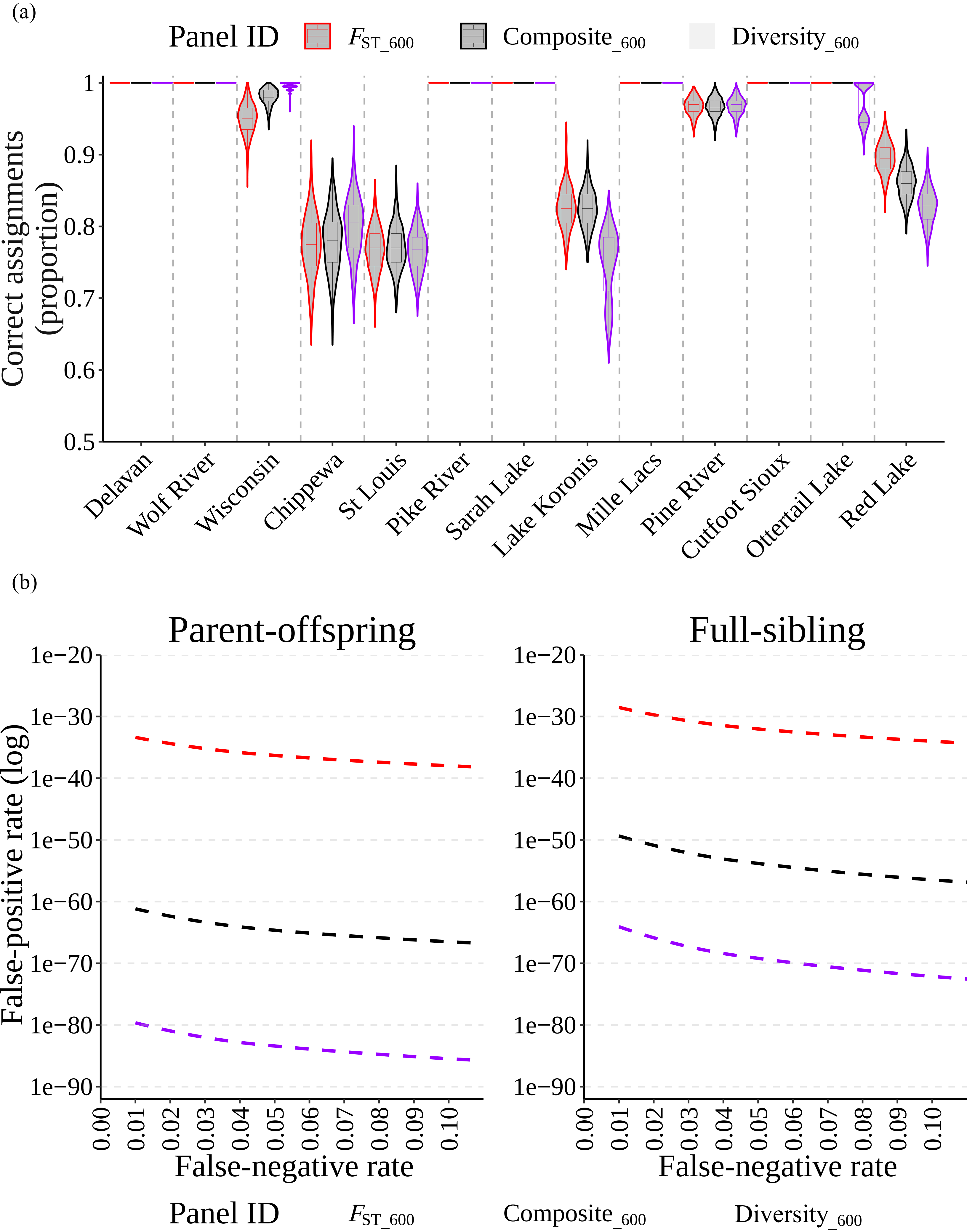
(a)
Panel ID
F_{ST_600}
Composite$_{\_600}$
Diversity$_{\_600}$
Correct assignments (proportion)
1
0.9
0.8
0.7
0.6
0.5
Delavan
Wolf River
Wisconsin
Chippewa
St Louis
Pike River
Sarah Lake
Lake Koronis
Mille Lacs
Pine River
Cutfoot Sioux
Ottertail Lake
Red Lake
(b)
Parent-offspring
Full-sibling
False-positive rate (log)
1e−20
1e−30
1e−40
1e−50
1e−60
1e−70
1e−80
1e−90
0.00
0.01
0.02
0.03
0.04
0.05
0.06
0.07
0.08
0.09
0.10
False-negative rate
Panel ID
F_{ST_600}
Composite$_{\_600}$
Diversity$_{\_600}$

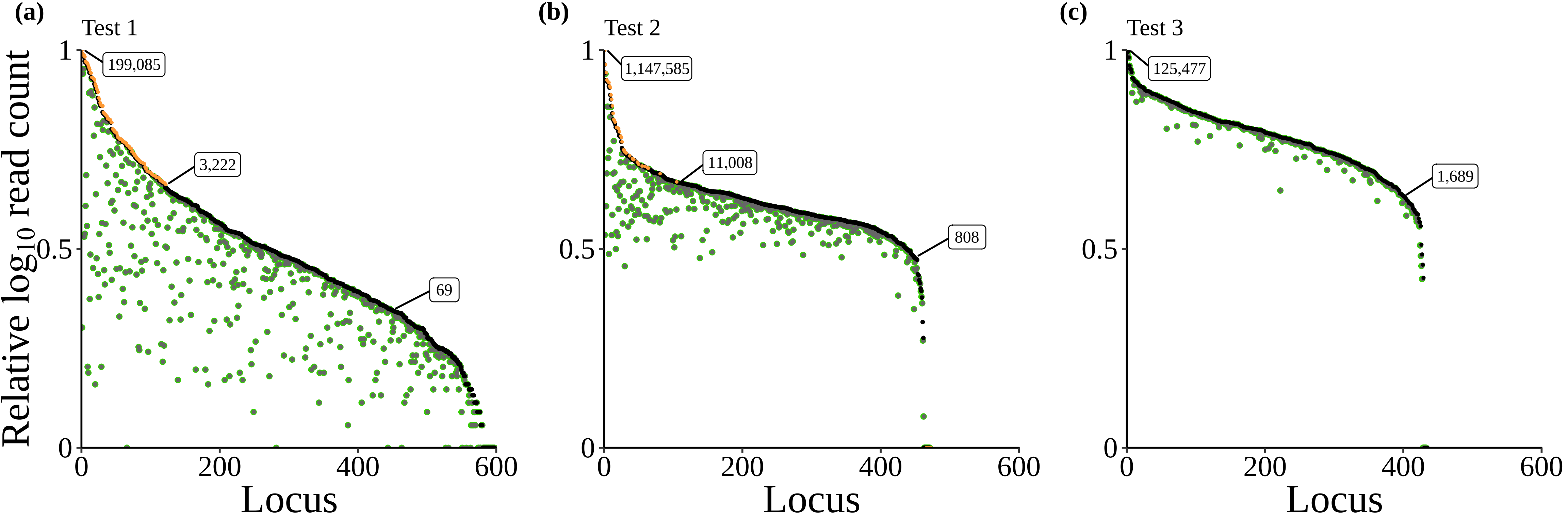
(a)
Test 1
Relative $\log_{10}$ read count
1
0.5
0
199,085
3,222
69
0
200
400
600
Locus
(b)
Test 2
1
0.5
0
1,147,585
11,008
808
0
200
400
600
Locus
(c)
Test 3
1
0.5
0
125,477
1,689
0
200
400
600
Locus

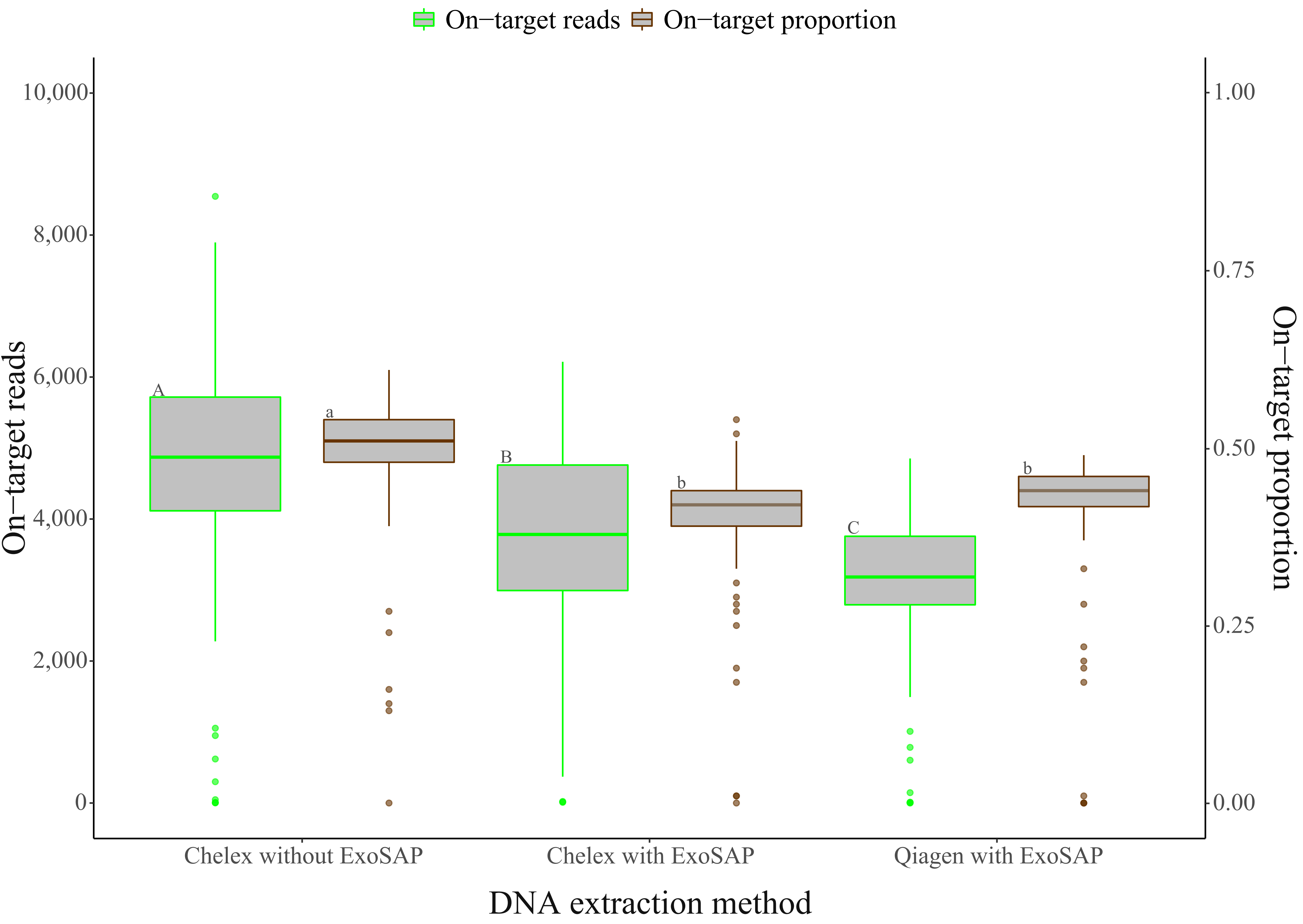
On−target reads
On−target proportion
10,000
8,000
6,000
4,000
2,000
0
1.00
0.75
0.50
0.25
0.00
On−target reads
On−target proportion
A
a
B
b
C
b
Chelex without ExoSAP
Chelex with ExoSAP
Qiagen with ExoSAP
DNA extraction method

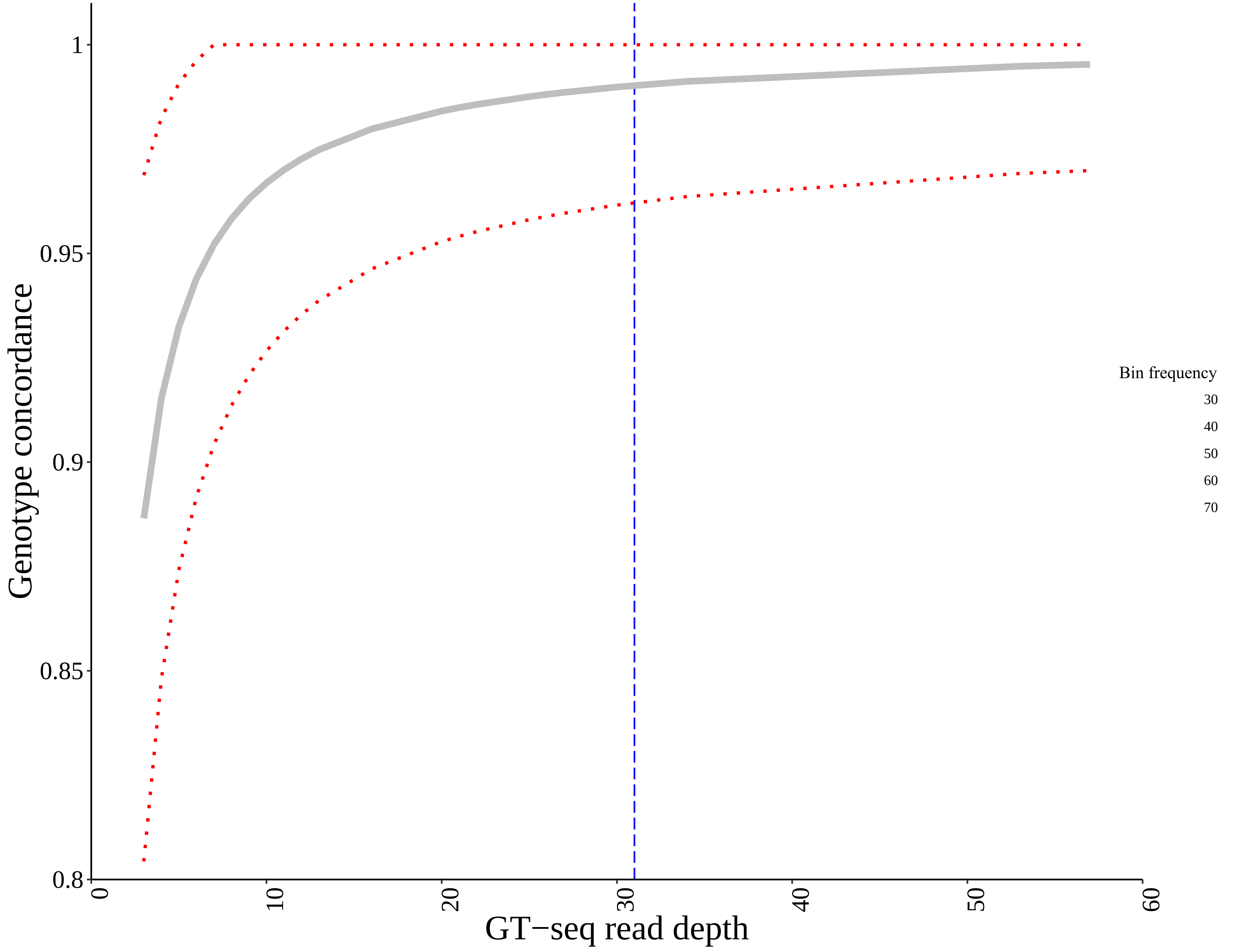
Genotype concordance
1
0.95
0.9
0.85
0.8
0
10
20
30
40
50
60
GT−seq read depth
Bin frequency
30
40
50
60
70

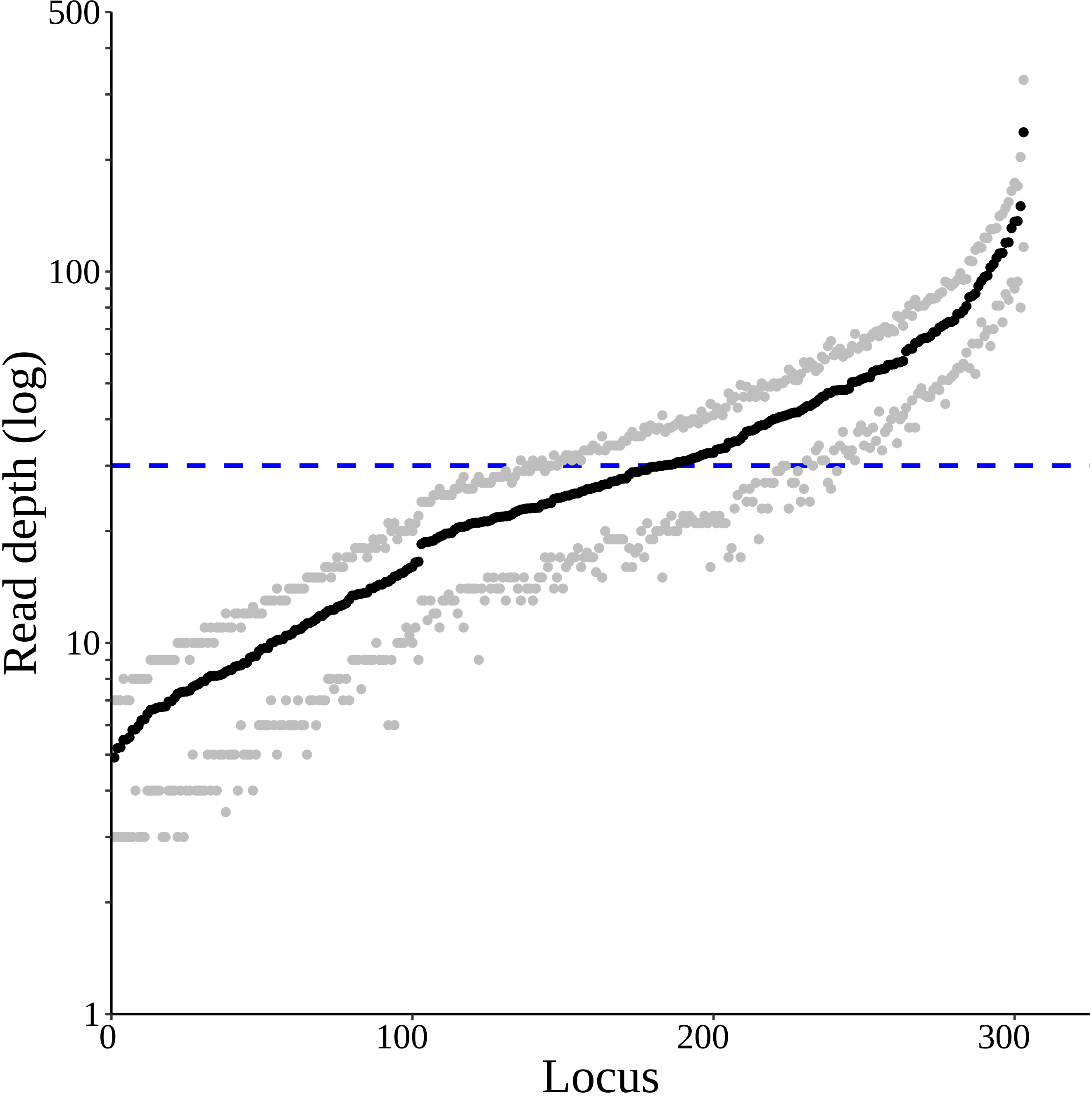

500
100
10
1
Read depth (log)
0
100
200
300
Locus